

Sara Sofie Øverbø Lindegård

Using a cellular metal structure to improve the thermal performance of a latent heat storage system

A numerical study

Master's thesis in Energy and environment

Supervisor: Erling Næss, Alexis Sevault

June 2020

Sara Sofie Øverbø Lindegård

Using a cellular metal structure to improve the thermal performance of a latent heat storage system

A numerical study

Master's thesis in Energy and environment
Supervisor: Erling Næss, Alexis Sevault
June 2020

Norwegian University of Science and Technology
Faculty of Engineering
Department of Energy and Process Engineering



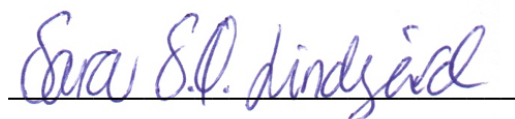
Preface

This report presents my Master's thesis at the Department of Energy and Process Engineering at the Norwegian University of Science and Technology (NTNU). The work counts 30 ECTS credits and concludes a Master's Degree program in Energy and Environment. During my thesis I have studied different elements of a cellular metal structure, for the purpose of enhancing the thermal performance of a latent heat storage system. I became familiar with phase change materials and latent heat storage systems when working on my Bachelor's thesis, and was intrigued by the potential for more efficient and environmentally friendly energy use.

Throughout my thesis work, I have received helpful guidance from my supervisors; Professor Erling Næss at NTNU and Research Scientist Alexis Sevault from SINTEF Energy Research. Thank you for your professional input and for always finding the time to answer my questions. Furthermore, I would like to thank Senior Engineer Inge Håvard Rekstad at NTNU for discussing practical implementation of the latent heat storage design, and Department Engineer Stein Kristian Skånøy for helping me in the laboratory.

The thesis will take part in the project PCM-Eff, supported by SINTEF Energy. I am humbled and grateful for the opportunity to contribute to this research, and hope the work will be found interesting.

Trondheim, June 11, 2020



Sara Sofie Øverbø Lindegård

Thesis description

Latent Heat Storage (LHS) represents an interesting concept of temporary thermal energy storage in many applications. Phase Change Materials (PCMs) are used as storage materials and the concept is based on heat absorption when the material undergoes a phase change, usually from solid to liquid, and subsequent heat release when the phase change is reversed. This allows for high energy density and low weight of the storage system compared to traditional sensible thermal energy storage. Though many PCM materials are well documented in the literature, their implementation is still limited due to the complexity of designing suitable interfaces between PCM, heat source and heat sink.

Batch combustion in wood log stoves is a promising application for LHS, due to the transient heat release with high peak values that need to be dampened. The purpose of the master project is to investigate a compact, passive, durable LHS system storing a substantial part of the heat release during domestic batch wood combustion, and effectively releasing the stored heat to the room for an extended period after the last batch. The following tasks are to be considered:

1. Literature review, focusing on calculation of heat distribution in heterogeneous materials, with the purpose of estimating effective/apparent thermal conductivities of PCMs having embedded metal structures for heat transfer enhancement.
2. A design of an improved latent heat storage system shall be developed, based on the experience acquired with the first prototype tested in the project work. A key factor in the new design is to improve the heat distribution inside the PCM storage.
3. A numerical analysis of the heat distribution in a PCM having an embedded cellular metal structure shall be conducted, using the CFD tool ANSYS Fluent for numerical simulations. Different design elements of the metal structure shall be investigated. Results shall be presented and discussed as well as proposal for further improvements on the LHS performance.
4. Proposals for further work shall be made.

Abstract

Thermal energy storage has the potential for more efficient and environmentally friendly energy use, as it allows for excess thermal energy to be stored and used at a later time. With the transient heat release of wood stoves, a discrepancy between heat demand and available thermal energy is not uncommon, and sensible heat storage in combination with wood stoves are widely used. The use of phase change materials (PCM) for latent heat storage (LHS) together with wood stoves is a lesser explored, yet promising concept. A latent heat storage system can have a more compact and lightweight design than a traditional heat storage, due to the large storage capacity per volume unit of phase change materials. However, the practical implementation of the concept is not without challenges.

This thesis aims to improve the thermal performance of a latent heat storage unit, for use in combination with wood stoves, with high-density polyethylene (HDPE) as PCM. Utilizing a cellular metal structure to enhance the heat transfer to the storage has been investigated through numerical analysis, using CFD software ANSYS Fluent. Wire thickness, pore size and porosity of metal structures have been evaluated with regards to their effect on heat distribution in metal structure/PCM-composites. Practical aspects and challenges have also been considered.

Two geometries were used for simulations: A cylinder of PCM with a wire along the center line, and a cellular structure filled with PCM. The cylinder had a 10 mm diameter and was 100 mm long. Wire diameters of 0.5 mm, 1 mm and 2 mm were investigated. The cellular structure had a wire diameter of 1 mm and cell width of 14 mm. Copper, aluminum, nickel, cast iron and stainless steel were evaluated as structure materials.

The numerical analysis concludes that good upward heat conduction in the metal structure is important to achieve sufficiently high temperatures to melt the PCM at the top of the structure. Wire diameter to structural height ratio is important in this regard, as is the thermal conductivity of the structure material. The latter also affects the storage capacity of the LHS system, as a structure with high thermal conductivity can have a higher porosity and thereby contain more PCM. Pore size must be seen in relation to wire thickness and thermal conductivity of the structure, as the rate at which the PCM melts, varies depending on the temperature of the metal structure.

Using cellular structures in combination with high-density polyethylene pose for several practical challenges, which to a large extent is related to the texture of melted high-density polyethylene. The numerical analysis show potential for enhanced heat transfer using metal structures, however, it is recommended to investigate alternative phase change materials, having a more liquid consistency, if choosing to proceed with cellular structures.

Sammendrag

Termisk energilagring har potensial for mer effektiv og miljøvennlig energibruk, ved at overflødig varme lagres til senere bruk. Ved vedfyring er det ikke uvanlig at tilgjengelig varme overstiger varmebehovet og varmelagring, ved bruk av tunge materialer, går langt tilbake i tid. Bruk av faseendringsmaterialer (PCM) for varmelagring i latente varmelagre (LHS) sammen med vedovn, er et lovende konsept. Et latent varmelager kan være lettere og mer kompakt enn et tradisjonelt varmelager, på grunn av materialers store lagringskapasitet per volumenhet under faseendring. Den praktiske implementeringen er imidlertid ikke uten utfordringer.

Arbeidet presentert i denne rapporten har hatt som mål å forbedre den termiske ytelsen til et latent varmelager, for bruk i kombinasjon med vedovn. Det aktuelle faseendringsmaterialet er "high-density polyethylene" (HDPE). Gjennom numerisk analyse har det blitt undersøkt å benytte en celleformet metallstruktur for å forbedre varmeoverføringen til lageret. Fokuset har vært på hvordan varmefordelingen i en metallstruktur/PCM-kompositt påvirkes av cellestørrelse, tykkelse på metalltråd og volumforhold mellom PCM og metall. Praktiske aspekter og utfordringer ved konstruksjon av et slikt lager har også blitt vurdert.

Programmet ANSYS Fluent ble benyttet til å utføre CFD simuleringer av to ulike geometrier: En enkelt metalltråd omringet av en sylinder av PCM og en cellestruktur fylt med PCM. Sylindere hadde en diameter på 10 mm og var 100 mm høy. Metalltråder med diametere på 0.5 mm, 1 mm og 2 mm ble undersøkt. Cellestrukturen hadde en tråddiameter på 1 mm og en maksimal cellestørrelse på 14 mm. Kobber, aluminium, nikkel, støpejern og rustfritt stål har blitt vurdert som strukturmateriale.

Den numeriske analysen konkluderer med at god varmeledning oppover i metallstrukturen er viktig for å oppnå tilstrekkelig høye temperaturer til å smelte PCMet på toppen av strukturen. Forholdet mellom tråddiameter og strukturhøyde er viktig i dette henseende, og det samme er strukturmaterialets termiske konduktivitet. Det sistnevnte påvirker også lagringskapasiteten til LHS systemet, ettersom en kompositt med høy effektiv termisk konduktivitet kan ha en mindre andel metall og derav en større andel PCM. Størrelsen på cellene må sees i sammenheng med tykkelsen på metalltrådene og den termiske konduktiviteten i strukturen, da smeltehastigheten i PCMet avhenger av temperaturen på metallstrukturen.

Det er flere praktiske utfordringer med å kombinere en cellulær struktur med HDPE. Dette skyldes i stor grad at HDPE blir svært lite flytende når det smelter. Den numeriske analysen viser potensial for forbedret varmeoverføring ved bruk av metallstrukturer, men det anbefales å undersøke alternative faseendringsmaterialer, med mer flytende konsistens, dersom det er ønskelig å benytte en cellestruktur.

Contents

Abstract	iii
Sammendrag	v
List of figures	viii
List of tables	xi
Nomenclature	xii
1 Introduction	1
1.1 Background	1
1.1.1 Previous design and experimental testing of the concept	2
1.2 Objective	2
1.3 Structure of the report	2
1.4 A brief introduction to high-density polyethylene used as a PCM to store thermal energy	3
1.5 An introduction to cellular metal structures and their potential for heat transfer enhancement in a composite	4
2 Literature review: Calculating effective thermal conductivity in heterogeneous materials	6
3 Methodology	10
3.1 Designing a latent heat storage unit for experimental testing	10
3.1.1 Calculations regarding porosity and pore size of a cellular metal structure	10
3.1.2 Laboratory testing as a part of the design process	14
3.1.3 Researching manufacturing methods and available metal structures	14
3.2 Numerical analysis	15
3.2.1 Geometry	15
3.2.2 Meshing	18
3.2.3 ANSYS Fluent setup	18
3.2.4 Data processing	19
4 Results	21
4.1 Design of an experimental heat storage unit	21
4.1.1 Exterior design	21
4.1.2 Metal structure design	23

4.2	Results from CFD simulations of case A: A single wire	28
4.2.1	Effect of wire thickness on PCM melting process	28
4.2.2	Effect of heat transfer area on PCM melting process	35
4.2.3	Effect of wire temperature on PCM melting process	36
4.3	Results from CFD simulations of case B: Metal structure	37
4.3.1	Melting process in a 10.8 cm tall metal structure/PCM composite .	37
4.3.2	Melting a layer equal the height of one metal cell	40
4.3.3	Effect of metal structure thermal conductivity on PCM melting process	42
4.3.4	Effect of contact area between metal structure and heat source on PCM melting process	43
5	Discussion	45
5.1	Discussion regarding experimental design	45
5.1.1	Discussion regarding design of metal structure	45
5.2	Discussion case A	47
5.2.1	Wire thickness	47
5.2.2	Pore size	48
5.3	Discussion case B	49
5.3.1	Porosity	49
5.3.2	Practical challenges	50
5.3.3	Heat distribution in a metal structure/PCM composite	51
5.4	Discussion regarding limitations of the numerical models	51
5.4.1	Comparing analytical calculations of melt front development with numerical calculations	52
6	Conclusion	54
6.1	Further work	55
	Bibliography	57
	A Original thesis description	60
	B Numerical model from preliminary project work	62
	C Quotation for production of metal foam, Goodfellow	65
	D Metal structure specifications discussed with SINTEF Industry	67
	E Metal structure specifications discussed with Tronrud Engineering	69

List of Figures

3.1	Illustration to accompany a description of calculating the melt front development in a PCM.	13
3.2	Case A: Geometry of a PCM cylinder with a wire along the center line. . .	15
3.3	Case B: Geometry and dimensions of one cell in a cellular metal structure.	16
3.4	Case B: Geometry of a cellular metal structure/PCM composite used for CFD simulations.	17
3.5	XY-section of case A geometry, illustrating a simplification used during post processing of data.	20
4.1	Design of a latent heat storage container	21
4.2	Latent heat storage container dimensions	22
4.3	Estimated relationship between effective thermal conductivity and PCM melting time	23
4.4	Effective thermal conductivity of cellular metal structures made out of copper, aluminum, nickel and cast iron as a function of porosity.	24
4.5	Development of the melt front in a PCM in radial direction	24
4.6	Pictures of high-density polyethylene during melting	26
4.7	Liquid fraction of high-density polyethylene as a function of time	29
4.8	Liquid-solid state of high-density polyethylene after one hour simulation flow time	29
4.9	Temperature profile of aluminum wire	31
4.10	Heat flux of aluminum wire to surrounding PCM	31
4.11	Development of PCM melt front in radial direction at different positions above heat source	33
4.12	Liquid-solid state of high-density polyethylene at different hours during melting	34
4.13	Effect of heat transfer area on PCM melting time	35
4.14	Effect of wire temperature on PCM melting time	36
4.15	Liquid fraction of high-density polyethylene with embedded cellular metal structure as a function of time at different positions above heat source . . .	38
4.16	A part of an aluminum structure/PCM composite, with section planes marking the widest part of the cells.	38
4.17	Temperature along the wires of a cellular metal structure	39
4.18	Liquid fraction of high-density polyethylene with embedded cellular metal structure as a function of time at different positions above bottom plate, a single cell	40
4.19	One metal structure cell with section planes marking different positions . .	41

4.20 XY-sections of a metal structure/PCM composite after 20 minutes heat supply	41
4.21 Effect of metal structure thermal conductivity on PCM melting time . . .	42
4.22 Cell orientations	44
4.23 Effect of contact area between metal structure and heat source on PCM melting time	44
5.1 Comparison of analytical and numerical calculations regarding radial melt front development	53
B.1 Boundary condition of container bottom used in 2D simulations	63
E.1 CAD model of metal structure for 3D printing made by Tronrud Engineering.	70

List of Tables

- 1.1 Thermal properties of high-density polyethylene 4
- 2.1 Empirical correlations modeling effective thermal conductivity of cellular metal structures. 7
- 3.1 Input data ANSYS Fluent: Thermal properties of high-density polyethylene 18
- 3.2 Input data ANSYS Fluent: Thermal properties of aluminum, copper and stainless steel. 19
- 4.1 Quotations for metal structures 27
- 4.2 Specifications regarding results in section 4.2.1 28
- 4.3 Specifications regarding results in section 4.2.1 30
- 4.4 Specifications regarding results in section 4.2.1 32
- 4.5 Specifications regarding results in section 4.2.2 35
- 4.6 Specifications regarding results in section 4.2.3 36
- 4.7 Specifications regarding results in section 4.3.1 37
- 4.8 Specifications regarding results in section 4.3.2 40
- 4.9 Specifications regarding results in section 4.3.3 42
- 4.10 Specifications regarding results in section 4.3.4 43
- B.1 Input data for 2D CFD simulations 64

Nomenclature

c_p	Specific heat capacity (J/kg·K)
d_0	Wire diameter (m)
H	Position above bottom of geometry (m)
k	Thermal conductivity (W/m·K)
k_{eff}	Effective thermal conductivity (W/m·K)
k_f	Thermal conductivity of substance filling the pores of a cellular metal structure (W/m·K)
k_l	Thermal conductivity of a substance in liquid state (W/m·K)
L	Length (m)
L_s	Latent heat of fusion (J/kg)
Q	Thermal energy per unit wire length (J/m)
q	Rate of thermal energy per unit wire length (W/m)
R_1	Thermal resistance of melted PCM layer (mK/W)
r	Radius (m)
r_m	Melt front position in radial direction (m)
r_0	Wire radius (m)
t	Time (s)
T	Temperature (°C)
T_0	Initial temperature (°C)
T_{deg}	Thermal degradation temperature (°C)
T_{melt}	Melting temperature (°C)
T_{sol}	Solidification temperature (°C)
x	Position in axial direction (m)

Greek letters

α	Thermal diffusivity (m ² /s)
ε	Metal structure porosity (-)
ρ	Density (kg/m ³)

Abbreviations

CFD	Computational Fluid Dynamics
HDPE	High-Density Polyethylene
LHS	Latent Heat Storage
PCM	Phase Change Material

Subscripts

$hdpe,s$	property related to solid HDPE
i	represents a time step
s	property related to a solid metal

Chapter 1

Introduction

1.1 Background

Thermal energy storage allows for excess thermal energy to be stored and used at a later time. This holds a potential for more efficient and environmentally friendly energy use. The batch combustion of wood stoves provides a transient heat release, which can result in the release of more heat at once than necessary. Utilizing a thermal energy storage can dampen the peaks and provide a more comfortable thermal environment as well as a smarter exploitation of the wood logs. Traditionally, when storing thermal energy from wood stoves, heat is stored in the thermal mass of heavy materials, such as soapstone or other type of rock. After the fire has burned out, heat will be transferred to the room from the warm stone for an extended time period.

A latent heat storage (LHS) system has the potential of providing a similar behavior, only utilizing the latent heat¹ during phase change of a material for storing heat from the combustion, rather than the sensible heat². During phase change, materials can store 5-14 times the amount of energy per volume that can be stored as sensible heat [1]. From this it follows that a LHS system can have a more compact and lightweight design than what is possible when using traditional sensible heat storage materials. As a part of their project PCM-Eff, SINTEF Energy Research are investigating this concept[2][3][4][5], using high-density polyethylene as the storing phase change material (PCM).

¹Latent heat - energy absorbed or released by a substance during its phase change, happening at more or less constant temperatures.

²Sensible heat - the energy required to change the temperature of a substance with no phase change.

1.1.1 Previous design and experimental testing of the concept

In relation to his master thesis at NTNU, Henning H. Mathisen developed a test design of a latent heat storage unit for use in combination with wood stoves [6]. The design was used for testing the concept and gathering experimental data regarding the thermal performance of such a system. The first prototype was a steel container with the shape of a quarter of a coaxial cylinder, designed to hold 4.8 kg of PCM. However, during testing, the unit did only contain 2.3 kg HDPE, which equals a PCM layer of 65 mm. The latent heat storage is imagined placed on top of the wood stove. Consequently heat is supplied through the bottom of the storage container. To portray the wood stove top for supplying heat to the system during testing, a heating plate was made out of copper and heat tape.

Experimental testing during a preliminary project work, found that it took more than six hours from the time heating was initiated until the PCM was completely melted, which was regarded as an inadequate charging time. Cooling down and solidifying the PCM was an even more time consuming process, and it was considered necessary with some sort of heat transfer enhancement measure [7].

1.2 Objective

This thesis will continue to investigate a compact, passive LHS system, for storing a substantial part of the heat release during domestic batch wood combustion. The objective of the thesis is to explore the potential of utilizing a cellular metal structure as heat transfer enhancement measure for improving the thermal performance of a LHS system.

Initially, the intention was to perform an experimental investigation of the potential of metal cell structures. A LHS design for experimental testing has been developed based on the experience acquired with the first prototype, tested in the preliminary project work. Due to the closing of laboratories at NTNU as a measure of infection prevention in relation to covid-19, the design has not been built or tested experimentally. Instead, a numerical approach has been used, performing simulations using CFD software ANSYS Fluent. The numerical analysis considers the heat distribution in a cellular metal structure and how this is affected by the design of the structure. The original thesis description can be found in appendix A.

1.3 Structure of the report

It is assumed that the reader has a general knowledge in thermal energy engineering and is familiar with the concept of phase change materials. The remaining part of this chapter will give an introduction to the material used as energy storage material, high-density

polyethylene, as well as an introduction to cellular metal structures and using them for heat transfer enhancement. Chapter two presents a literature review on calculating effective thermal conductivity in heterogeneous material. Insight gathered from the literature study is used when designing the metal structure of the LHS system.

The first part of chapter three presents the process of designing the LHS unit for experimental testing. This was done primary to the numerical analysis and involved analytical calculations, 2D simulations, laboratory testing and researching manufacturing methods. The second part of the chapter lays out the background information and procedure of the CFD simulations used for numerical analysis.

Results are presented in chapter four. The first part considers the results from the calculations, laboratory tests and research of the design process and presents the LHS design. Then follows the results of the CFD simulations, divided into case A and case B. The results are discussed in chapter five. The chapter elaborates upon choices made in regards to the LHS design as well as challenges during the design process. The results from the numerical simulations are discussed in regards to improving the thermal performance of a LHS system. Furthermore, the chapter includes a discussion regarding the set up of the numerical models. Chapter six concludes the discussion and provides suggestions for further work.

1.4 A brief introduction to high-density polyethylene used as a PCM to store thermal energy

High-density polyethylene (HDPE) is a type of plastic used in a wide range of applications, for instance in bottles and pipes. It is easily available and inexpensive. Its melting temperature is approximately 130°C and it starts to solidify at 125°C. The thermal degradation temperature of HDPE is 300°C. As it is desirable for the LHS to be durable, it is important that the storage material can undergo a number of phase change cycles without changing its properties. The thermal degradation temperature therefore puts an upper limit to the temperature the storage can withstand.

During melting, HDPE can store 152 kJ/kg. Approximating the density to be 1000 kg/m³, this equals a storage capacity of 152 · 10³ kJ/m³. For comparison, soapstone has a sensible storage capacity of 3 · 10³ kJ/m³/K. Assuming that melting happens during a temperature rise of 5°C, HDPE can store 10 times the energy per volume during melting as can be stored as sensible heat using soapstone.

When searching for a suitable PCM, several properties are evaluated. Sevault et al. presents key indicators for choosing a good PCM in *PCMs for thermal energy storage*

in low- and high-temperature applications: a state-of-the-art [4]. HDPE possess many favorable properties, such as appropriate phase change temperatures and high latent heat per volume unit. However, few, if any, materials meet all the criteria of a perfect PCM. Low thermal conductivity is often an unwanted characteristic, as is the case for HDPE. The consequence is large temperature gradients within the material and slow charging and discharging of the energy storage. Furthermore, HDPE is a highly viscous substance. Numbers regarding the viscosity is missing, but results from laboratory tests suggest that free convection in the melted material is non-existing, due to the consistency of the material. This pose for challenges designing a LHS system with good thermal performance, which this thesis aims to ease. Thermal properties of HDPE is summarised in table 1.1.

Table 1.1: Thermal properties of high-density polyethylene in solid and liquid state [6].

Thermal property	Unit		Value
Density, ρ	$\text{kg}\cdot\text{m}^{-3}$	solid (25°C)	960
		liquid (150°C)	802
Specific heat capacity, c_p	$\text{J}\cdot(\text{kg}\cdot\text{K})^{-1}$	solid average	2200
		liquid average	2700
Thermal conductivity, k	$\text{W}\cdot(\text{m}\cdot\text{K})^{-1}$	solid (25°C)	0.55
		liquid (150°C)	0.21
Latent heat of fusion, L_s	$\text{J}\cdot\text{kg}^{-1}$		$152\cdot 10^3$
Melting temperature, T_{melt}	°C		129 - 134
Solidification temperature, T_{sol}	°C		122 - 125
Thermal degradation temp., T_{deg}	°C		300

1.5 An introduction to cellular metal structures and their potential for heat transfer enhancement in a composite

Metal foams are cellular structures where solid metal makes up typically 5-25% of the volume, while the rest is voids that can be filled with a different substance. A foam can be open-celled or closed and the distribution of the cells can be random or ordered. The term foam is often associated with a random cell distribution. As this thesis will consider both random and ordered foams, the term metal structure will be used instead.

With their low density and good heat conducting abilities, cellular metal structures hold the potential for keeping a design compact and lightweight, while improving the transportation of heat through a material with poor thermal conductivity [8]. Siapush et al. [9] used a copper foam of 95% porosity and a pore size between 0.13 and 2.5 mm to increase the thermal conductivity of a PCM from 0.423 W/mK to 3.06 W/mK. Porosity refers to the percentage of the volume that is not occupied by metal, which means that in the study of Siapush et al., the thermal conductivity increased drastically by incorporating only 5% copper.

However, porosity is not the whole story. Pore size and wire thickness are design parameters that have been studied and shown to affect the performance of the structure. Zhong et al. [10] did a study with graphite structure and paraffin wax and found that a small pore size and large wire diameter in the structure gives a higher thermal diffusivity. On the other hand, larger pore size and thinner wires give a better latent heat storage capacity. They concluded that high storage capacity and high thermal diffusivity can be achieved by using a structure with thicker wires and larger pore size.

Lafdi et al.[11] studied the effect of pore size and structure porosity on the melting rate of paraffin wax, using an aluminum structure. They found that while a lower porosity increased the conduction in the composite, a higher porosity and bigger pore size accelerated the attainment of steady-state temperature, due to the higher effect of liquid phase convection motion.

Chapter 2

Literature review: Calculating effective thermal conductivity in heterogeneous materials

When designing a metal structure for enhancing the heat conduction through a PCM, it can be useful to know the effective thermal conductivity of the metal structure/PCM-composite. The effective thermal conductivity refers to the composite's ability to conduct heat when assimilated to a homogeneous medium. This chapter will present different models for calculating the effective thermal conductivity found in literature.

In general, conventional phase change materials possess low thermal conductivity. With this it follows that conduction through the material is slow, making the charging and discharging of the thermal energy storage slow. Combining a PCM with a high-porosity metal structure can increase the thermal performance of the storage[8][9][10][11]. It is common to treat the composite as a homogeneous medium having an effective thermal conductivity, k_{eff} . Several relationships describing the effective thermal conductivity of metal structures are available in literature. Ranut and Nobile [12] present a number of models and evaluate their accuracy by comparing the calculated values with experimental values found in literature. The models have been tested for cellular structures filled with air and water.

When estimating the effective thermal conductivity, there are two main ways of arranging the thermal conductivity of the metal, k_s , and the substance filling the pores, k_f , in relation to each other; in parallel and in series. The parallel model estimates k_{eff} as a weighted average based on the volume fraction, ε , of the metal and the pore filling, as presented in equation 2.1. The series model is represented by equation 2.2. According to Ranut and Nobile these models are not suited for describing the real trend of experimental data. However, with their simplicity they are easy to use.

CHAPTER 2. LITERATURE REVIEW: CALCULATING EFFECTIVE THERMAL
CONDUCTIVITY IN HETEROGENEOUS MATERIALS

$$k_{parallel} = k_{eff} = \varepsilon k_f + (1 - \varepsilon)k_s \quad (2.1)$$

$$k_{series} = k_{eff} = \left(\frac{\varepsilon}{k_f} + \frac{1 - \varepsilon}{k_s} \right)^{-1} \quad (2.2)$$

Empirical correlations have been developed combining the parallel and series models with fitting parameters, whose values are calibrated over experimental measurements. Calmidi and Mahajan [13] adjusted the parallel model and calibrated the fitting parameters according to their experimental data on aluminum foams with porosities higher than 90%. Bhattacharya et al. [14] as well as Singh and Kasana [15] combined the series and parallel method to express the effective thermal conductivity. The three correlations are presented in table 2.1.

Table 2.1: Empirical correlations modeling effective thermal conductivity of cellular metal structures.

Author	Model
Bhattacharya et al.[14]	$k_{eff} = Ak_{parallel} + (1 - A)k_{series}$ $A = 0.35$
Calmidi and Mahajan[13]	$k_{eff} = \varepsilon k_f + A(1 - \varepsilon)^n k_s$ $A = 0.181, n = 0.763$
Singh and Kasana[15]	$k_{eff} = k_{parallel}^F + k_{series}^{1-F}$ $F = C[0.3031 + 0.0623 \ln (\varepsilon k_s / k_f)]$ $0 \leq F \leq 1, C: \text{ depends on the substance filling the pores}$

Other models have been formulated using a unit cell approach. These are theoretical models based on an idealized, simplified foam geometry. A model is developed for a single unit cell, which is assumed to repeat itself throughout the composite. The shape of the cell, the geometry of the structure wires and how they are connected at their intersection differ between the models. Calmidi and Mahajan [13] developed a model based on a two-dimensional array of hexagonal cells, with square metal lumps at the wire's intersections. The layers of the geometry are arranged in series, while the metal and the pore filling

within each layer are arranged in parallel. Ranut and Nobile found that the model fits well with experimental data using air and water as pore filling. Siahpush et al. [9] studied the heat transfer enhancement of a 95% porosity copper foam in a latent heat storage system using eicosane as PCM, and showed that the model of Calmidi and Mahajan agreed within 3% of the experimental values for effective thermal conductivity. The model is presented in equation 2.3

$$k_{eff} = \left(\frac{2}{\sqrt{3}} \left(\frac{r \frac{b}{L}}{k_f + (1 + \frac{b}{L}) \frac{k_s - k_f}{3}} + \frac{(1-r) \frac{b}{L}}{k_f + \frac{2}{3} \frac{b}{L} (k_s - k_f)} + \frac{\frac{\sqrt{3}}{2} - \frac{b}{L}}{k_f + \frac{4r}{3\sqrt{3}} \frac{b}{L} (k_s - k_f)} \right) \right)^{-1} \quad (2.3)$$

where

$$\frac{b}{L} = \frac{-r + \sqrt{r^2 + \frac{2}{\sqrt{3}}(1-\varepsilon)(2 - r(1 + \frac{4}{\sqrt{3}}))}}{\frac{2}{3}(2 - r(1 + \frac{4}{\sqrt{3}}))},$$

$r = 0.09$ or $r = \frac{t}{b} < 0.0336$, b : half thickness of the lump, t : half thickness of the wire, L : length of the wire.

Yang et al. [16] suggested a simpler model based on a three-dimensional tetrakaidecahedron unit cell, assuming one-dimensional heat conduction along the wires of the cell and negligible conduction through the substance filling the voids of the structure. The porosity, ε , of the structure must be greater than 0.9, for the assumption of one-dimensional heat conduction to be valid. The model is presented in equation 2.4 and expresses the dependence of effective thermal conductivity on porosity, whereas the effect of pore size is not included.

$$k_{eff} = \frac{1}{3}(1 - \varepsilon)k_s \quad (2.4)$$

There are models predicting the effective thermal conductivity of composites, not developed specifically for metal structures, which, according to Ranut and Nobile, gives reasonable estimations of the thermal conductivity of metal structure/PCM-composites. Schuetz and Glicksmann (from [12]) developed an analytical model for polymeric foams with porosity above 95%. The only design dependent parameters are the porosity and the fraction of the solid phase in the cell structure, which for metal structures equals one. The model resembles the parallel model, but gives a better prediction, according to Ranut and Nobiles comparisons with experimental data. Dul'nev (from [12]) formed a model

CHAPTER 2. LITERATURE REVIEW: CALCULATING EFFECTIVE THERMAL CONDUCTIVITY IN HETEROGENEOUS MATERIALS

for disperse solid systems, based on a cubic unit cell, and Ahern et al. [17] developed a correlation based on Maxwell relation for mixtures of materials having different electrical conductivities, which both decently predicts the effective thermal conductivity of cellular metal structures. Equations describing these models are not presented in this report, but can be found in *On the effective thermal conductivity of metal foams* by Ranut and Nobile [12].

Chapter 3

Methodology

3.1 Designing a latent heat storage unit for experimental testing

Designing an improved latent heat storage unit for experimental testing has mainly involved designing a cellular metal structure. Only small adjustments have been made to the exterior design of the first prototype. The process of designing the metal structure has consisted of calculations on porosity and pore size, laboratory tests looking into practical challenges regarding filling the cells with PCM, as well as researching what is available in the market at what price.

3.1.1 Calculations regarding porosity and pore size of a cellular metal structure

Porosity

A 2D model, made in ANSYS Fluent, recreating the laboratory test conducted during the project work was used to estimate how the melting time of HDPE is affected by increased effective thermal conductivity. The geometry of the model is a 171x55 mm rectangle of HDPE, enclosed by a steel frame with insulation on top and one side. CFD simulations were run with input values for thermal conductivity of HDPE equal 1, 1.2, 1.5, 2, 2.2, 2.8 and 5 W/mK and the time it took to melt the HDPE in each case was registered. Further information about the numerical model can be found in appendix B.

The effective thermal conductivity as a function of porosity was estimated using the model of Yang et al. [16], represented by equation 3.1. The model is limited to structure porosities, ε , greater than 0.9 and assumes heat will only be conducted through the metal structure. k_s is the thermal conductivity of the solid metal of the structure.

$$k_{eff} = \frac{1}{3}(1 - \varepsilon) \cdot k_s \quad (3.1)$$

Pore size: Estimating the development of the melt front

Calculations on how the melt front of HDPE moves with time in radial direction, when heat is supplied from a wire with constant temperature, have been conducted. The illustrations in figure 3.1 accompanies the following description of the calculations. The wire has a radius, r_0 , and holds a constant temperature, T_s . Surrounding the wire is an infinite area of PCM, which at $t = 0$ is solid (figure 3.1a). Treating the wire as a plane wall with length $L = 2\pi r_0$ (figure 3.1b), the temperature distribution in the PCM with time can be expressed by equation 3.2, assuming that phase change does not occur.

$$\frac{T(x, t) - T_0}{T_s - T_0} = erf\left(\frac{x}{2\sqrt{\alpha t}}\right), \quad (3.2)$$

where T_0 is the initial temperature of the PCM and α is the thermal diffusivity of solid PCM. Equation 3.2 was used to determine the time it takes to raise the temperature from T_0 to melting temperature at position x . Some of the PCM between the wall and position x , will in reality melt during this time as the temperature reaches melting temperature.

Holding on to the assumption that the PCM does *not* start to melt, the amount of energy per unit wire length needed to heat a layer of thickness x from melting temperature T_{melt} to $\frac{T_s + T_{melt}}{2}$ ¹ was determined by equation 3.3.

$$Q = \rho_{hdpe,s} \cdot 2\pi r_0 \cdot c_{p,hdpe,s} \cdot \frac{T_s - T_{melt}}{2} \cdot x \quad (\text{J/m}) \quad (3.3)$$

Assuming that this energy goes into melting the PCM instead of raising the temperature above melting temperature, the thickness of the melted PCM layer was estimated by combining equation 3.3 and 3.4 (figure 3.1c). The latter expresses the energy needed to melt a layer of PCM of tickness $r_m - r_0$, where r_m is the position of the melt front in radial direction. L_s is the latent heat of fusion.

$$Q = \rho_{hdpe,s} \pi (r_m^2 - r_0^2) L_s \quad (\text{J/m}) \quad (3.4)$$

¹The average temperature of the PCM between the wall and position x , assuming a linear temperature profile.

With $x = 1$ mm, this approach was used to approximate the time, t_1 , of melting the first PCM layer. t_1 was set as the starting time for further calculations and the location of the melt front at t_1 equals $r_{m,1} = r_m$ from equation 3.4. For each time step, i , a new location of the melt front, $r_{m,i+1}$, was calculated using the following approach.

The melted PCM has a resistance $R_{1,i}$ expressed by equation 3.5.

$$R_{1,i} = \frac{\ln(r_{m,1}/r_0)}{2\pi k_l}, \quad (\text{mK/W}) \quad (3.5)$$

where k_l is the thermal conductivity of liquid PCM. The rate of heat transfer per unit wire length across the melted layer was modelled using equation 3.6.

$$q_{1,i} = \frac{T_s - T_{melt}}{R_{1,i}}, \quad (\text{W/m}) \quad (3.6)$$

Treating the melt front as a wall with length $L = 2\pi r_{m,i}$ and constant temperature equal T_{melt} , the heat transfer rate from the melted to the solid PCM was expressed by equation 3.7.

$$q_{2,i} = \frac{k_s(T_{melt} - T_0)}{\sqrt{\pi\alpha t_i} \cdot 2\pi r_{m,i}}, \quad (\text{W/m}) \quad (3.7)$$

The difference between $q_{1,i} \cdot \Delta t$ and $q_{2,i} \cdot \Delta t$ is the energy that goes into melting a new layer of PCM, moving the location of the melt front further away from the wire. Δt is the length of one time step, $\Delta t = t_i - t_{i-1}$, which was set to two seconds. The new location of the melt front was then determined by solving equation 3.8 with respect to $r_{m,i+1}$.

$$(q_{1,i} - q_{2,i})\Delta t = \rho\pi(r_{m,i+1}^2 - r_{m,i}^2)L_s \quad (3.8)$$

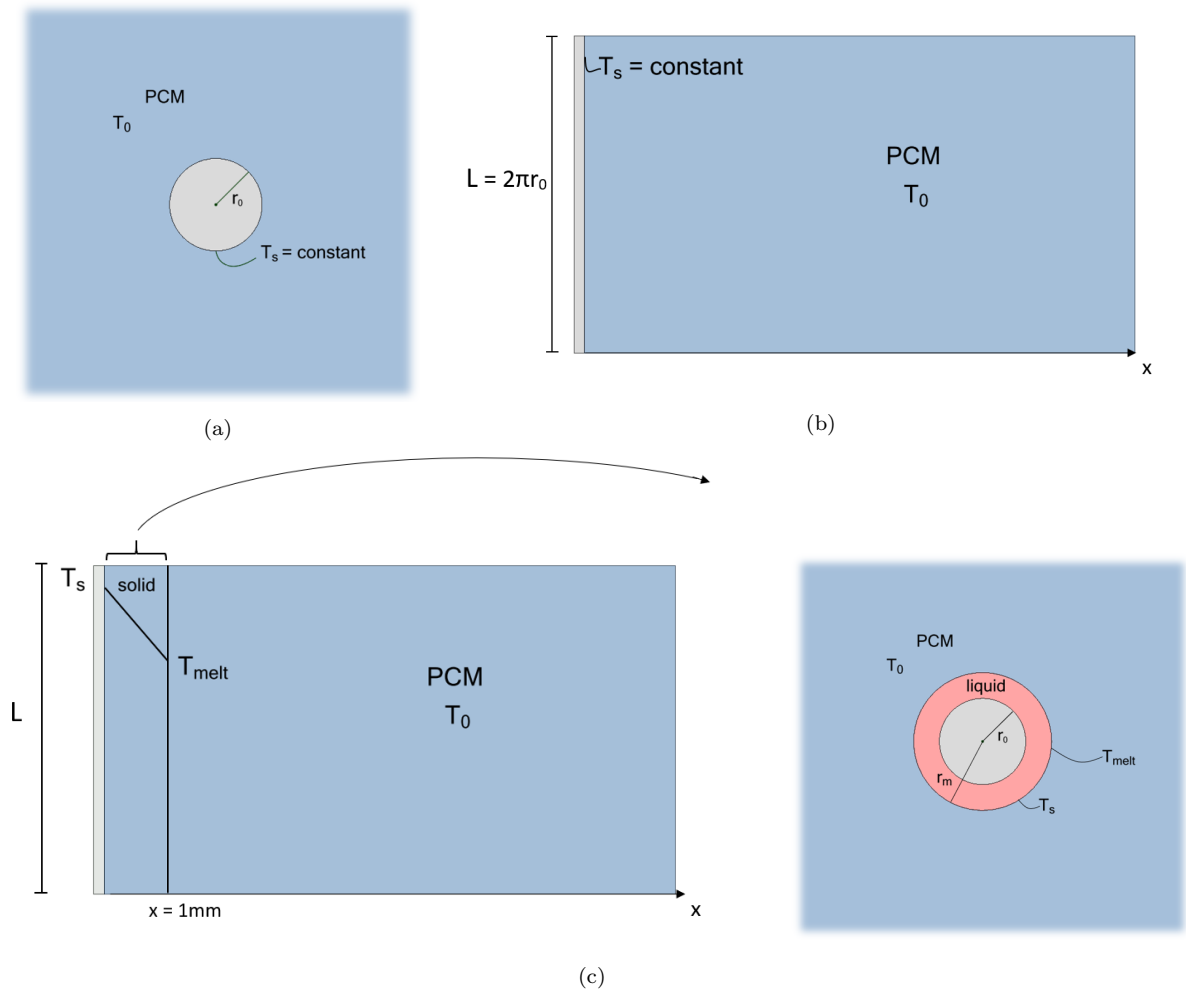


Figure 3.1: The illustrations accompany a description of estimating the development of the melt front in radial direction in a PCM.

3.1.2 Laboratory testing as a part of the design process

The texture of melted HDPE raises a question on how to fill the cells of the metal structure with HDPE in a satisfying manner, obtaining good connection between the metal and the PCM, leaving as little air as possible in the composite. To get a better understanding of the behaviour of HDPE when exposed to temperatures above its melting point, the material was heated in a saucepan placed on a hot plate.

The temperature of the hot plate was kept at either 140, 160 or 220°C for approximately two hours. The saucepan was covered by a lid, which occasionally was removed to inspect the melting process. The solid HDPE was in the shape of shavings before heating was initiated. From time to time during melting, the material was pushed down towards the bottom of the saucepan to make it more uniform and push out air bubbles.

It was attempted to combine the HDPE with an aluminum honeycomb structure using two different strategies. One was pushing the aluminum structure into melted HDPE and the other was to fill the structure with solid HDPE shavings and subsequently melt the PCM.

3.1.3 Researching manufacturing methods and available metal structures

Parallel with investigating design parameters of a metal structure, an analysis of what is available in the market was conducted. This included looking into what was available to order "ready-made", the possibility of getting a structure costume ordered and at what price. Suppliers were contacted by e-mail or phone.

3.2 Numerical analysis

Numerical models have been created using ANSYS software. CFD simulations were run using ANSYS Fluent 2019 R2 and the results of the simulations were analysed through the visualisation and analysis software Tecplot 360 EX.

ANSYS Fluent uses an enthalpy-porosity technique for modelling solidification and melting processes, as described in the Fluent Theory Guide [18]. The enthalpy formulation method is a widely used approach for solving heat transfer problems in melting and solidification processes [2][19][20]. Its major advantage is that it does not require explicit treatment of the moving solid-liquid boundary. In *Numerical modeling of a latent heat storage system in a stovepipe*[2], Sevault et al. gives a concise explanation of the theory behind modelling moving boundary problems and the equations used in ANSYS Fluent. The following sections of this chapter provides specifications regarding geometry, meshing, the numerical setup of the models and how data has been handled during post processing.

3.2.1 Geometry

Case A: A single wire

CFD simulations have been performed using two different geometries. Case A looks at a single wire surrounded by PCM. The geometry consists of two coaxial cylinders, where the inner cylinder has a diameter, d_0 , of either 0.5 mm, 1 mm or 2 mm. The outer cylinder has a diameter of 10 mm and the length is 100 mm. The geometry of case A with $d_0 = 1$ mm is displayed in figure 3.2.



Figure 3.2: Geometry used for CFD simulations of a PCM cylinder with a wire along the center line.

Case B: Cellular metal structure

Case B simulates an ordered, open celled metal structure with pores in the shape of tetrakaidecahedrons. The tetrakaidecahedron is also known as the Kelvin cell² and is a commonly used shape when modelling open celled structures [16][20][21]. The diameter of the cell wires are 1 mm and dimensions for one single cell are shown in figure 3.3. Simulations have been conducted with either three or eight cells stacked on top of each other. Figure 3.4 shows the geometry with the height of three cells. To reduce the necessary computational power, symmetry across the XZ- and YZ-plane was exploited, simulating only one fourth of the geometry shown in figure 3.4.

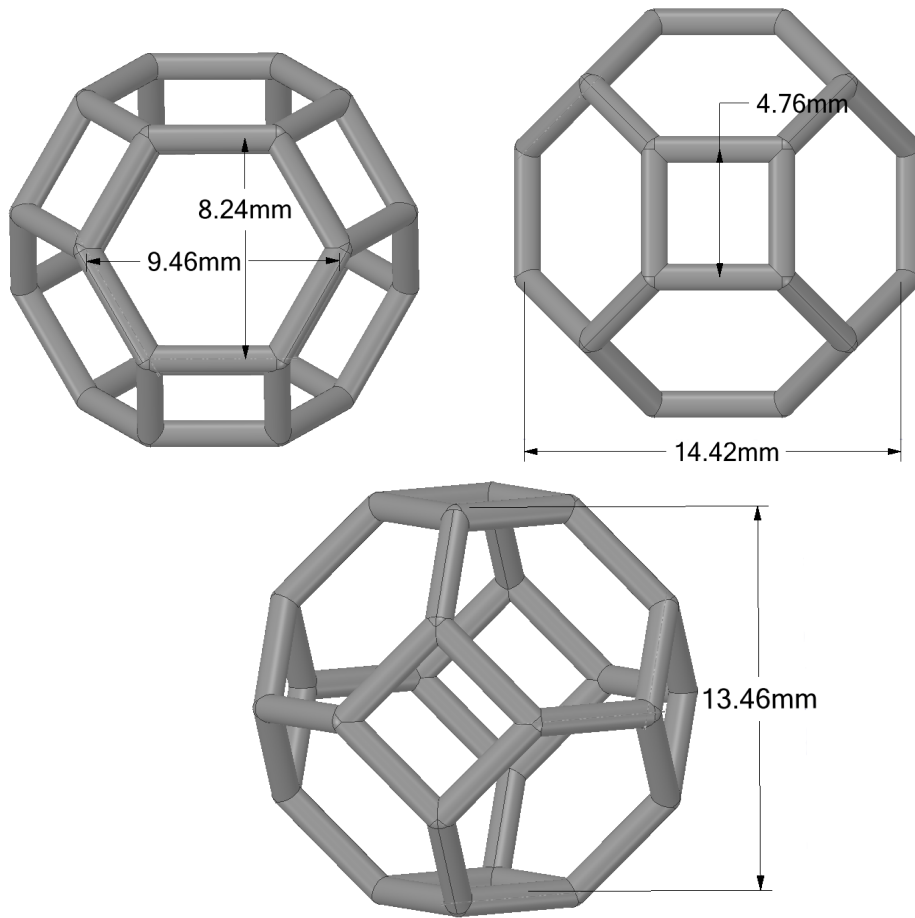


Figure 3.3: Tetrakaidecahedron cell with dimensions, used in CFD simulations modelling the heat distribution in a cellular metal structure/PCM composite.

²Known as one of the best shapes for packing equal-sized objects together to fill space with minimal surface area.

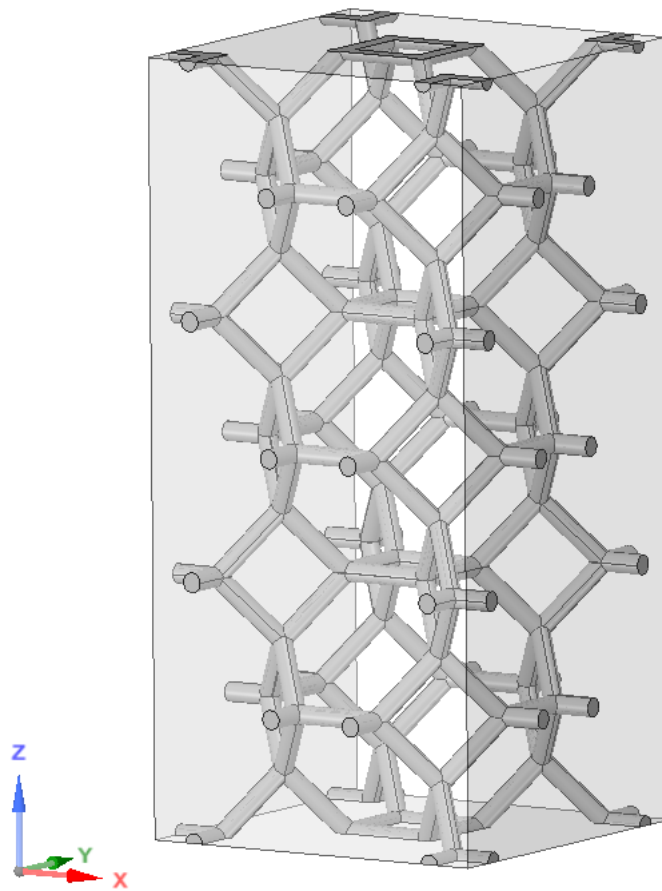


Figure 3.4: Geometry used for CFD simulations modelling the heat distribution in a cellular metal structure/PCM composite. The box encapsulating the cellular structure represents a PCM.

3.2.2 Meshing

Meshing was done using ANSYS Meshing. A mesh sensitivity analysis was conducted for case A, using four different mesh refinements of $5.7 \cdot 10^4$, $7.2 \cdot 10^4$, $9.9 \cdot 10^4$ and $1.1 \cdot 10^5$ elements, where the second finest mesh was used for further simulations. Approximately $3 \cdot 10^4$ elements per metal structure cell was used in case B.

3.2.3 ANSYS Fluent setup

Time was set to "Transient", solver type to "Pressure-based" and velocity formulation to "Absolute". The energy model and the solidification and melting model were turned on and the viscous model was set to "Laminar". The zones modelling PCM were defined as "fluid" and assigned the thermophysical properties of HDPE presented in table 3.1. Zones modelling the metal were defined as solid and given the thermophysical properties of either aluminum, copper or stainless steel, listed in table 3.2. Reference values were set to match the properties of HDPE and the PCM-zone was chosen as the reference zone. A time step of 0.1 second was used during the first ten minutes simulation flow time. For the rest of the simulations, a time step of one second was considered sufficient for predicting the behavior of the PCM.

Table 3.1: Input data for thermal properties of high-density polyethylene used for modelling in ANSYS Fluent.

Property	Unit	Value
Density	$\text{kg} \cdot \text{m}^{-3}$	960
Thermal Conductivity	$\text{W} \cdot (\text{m} \cdot \text{K})^{-1}$	0.21
Viscosity	$\text{kg} \cdot (\text{m} \cdot \text{s})^{-1}$	1000*
Specific Heat Capacity	$\text{J} \cdot (\text{kg} \cdot \text{K})^{-1}$	1890 - 2920**
Pure Solvent Melting Heat	$\text{J} \cdot \text{kg}^{-1}$	151 600
Solidus Temperature	K	402
Liquidus Temperature	K	407

* Information regarding the actual viscosity of HDPE is missing. A large value is chosen to indicate no convection motion.

** Piecewise-linear, ten points from 1890 J/kgK at 298 K to 2920 J/kgK at 523 K.

Table 3.2: Input data for thermal properties of aluminum, copper and stainless steel used for modelling in ANSYS Fluent.

Property	Unit	Value Al	Value Cu	Value Steel
Density	$\text{kg}\cdot\text{m}^{-3}$	2719	8978	8030
Thermal Conductivity	$\text{W}\cdot(\text{m}\cdot\text{K})^{-1}$	202.4	387.6	16.27
Specific Heat Capacity	$\text{J}\cdot(\text{kg}\cdot\text{K})^{-1}$	871	381	502

Boundary conditions

Two sets of boundary conditions were used for case A, one being constant temperature at the bottom of the geometry and the other; constant temperature over the entire wire (inner cylinder). The temperature was either set to 150, 200 or 250°C. The cylinder wall and top of the outer cylinder was defined as adiabatic, as was the bottom of the geometry when not held at a constant temperature. For case B all boundary conditions were set to adiabatic, except for the bottom of the geometry which was kept at a constant temperature of 250°C. The initial temperature of the systems was kept as default equal 27°C.

Solution methods and controls

Regarding solution methods, the "SIMPLE" scheme was used for the pressure-velocity coupling, "PRESTO!" was used for the pressure correction equation and the momentum and energy equations were computed using the "First order upwind" scheme. For solution control, the under-relaxation factors were set as following: Pressure = 0.3, density = 0.8, body forces = 1, momentum = 0.3, liquid fraction update = 0.1 and energy = 1.

3.2.4 Data processing

Fluent data files were saved every minute and subsequently uploaded to Tecplot 360 EX for 3D visualisation of what happened in the systems. Relevant data points regarding liquid fraction of HDPE, wire temperatures and boundary heat flux were extracted from Tecplot. MATLAB was used for creating graphical presentation of the data. In case A, the position of the melt front in radial direction was estimated from liquid fraction of XY-sections of the geometry. By assuming that the PCM was either completely melted or completely solid, an approximate position of the melt front was determined using the relationship in equation 3.9.

$$Liquid\ fraction = \frac{r_m^2 - r_0^2}{r_{cyl}^2 - r_0^2}, \quad (3.9)$$

where r_m is the position of the melt front in radial direction, r_0 is the wire radius and r_{cyl} is the radius of the cylinder.

Figure 3.5 shows a XY-section of the geometry in case A. Figure (a) shows the section as it was displayed in Tecplot, and figure (b) illustrates the section when assuming completely melted or completely solid material. Blue represents solid and red liquid, while the yellow and green shades indicate that the material is in transition between the two phases.

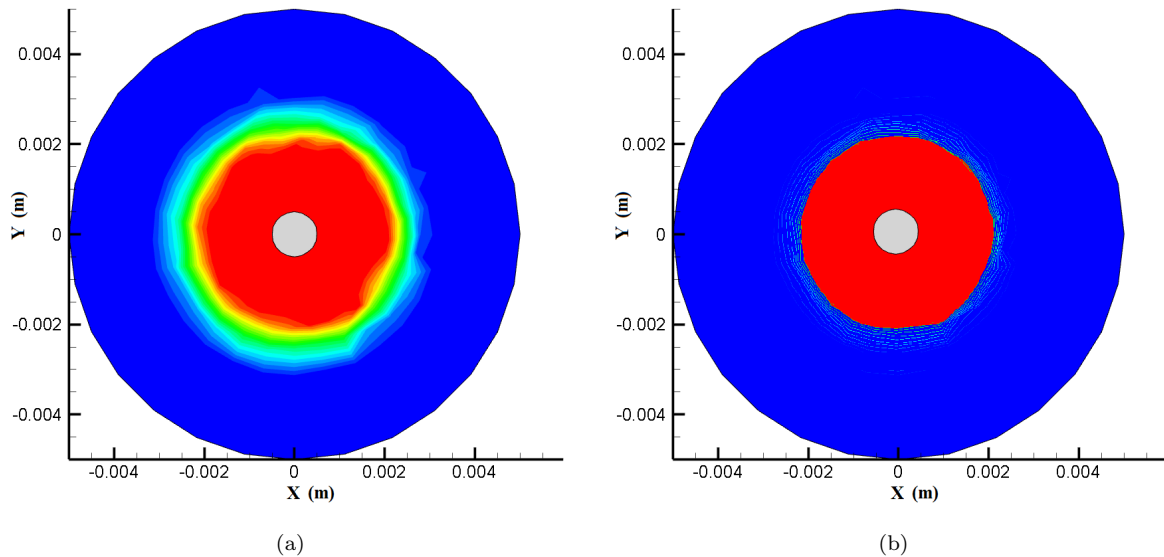


Figure 3.5: XY-section of a wire surrounded by a cylinder of PCM. (a) The state of the PCM during melting, as shown in the CFD post processing tool Tecplot 360 EX. Blue indicates solid material, red is liquid and the yellow and green shades represents material which is in transition between the two phases. (b) A simplification of the situation shown in figure (a) assuming that the material is either completely solid or completely liquid.

Chapter 4

Results

4.1 Design of an experimental heat storage unit

4.1.1 Exterior design

The exterior design of the storage unit is displayed in figure 4.1. The container has a volume of 4.7 L and is designed to hold 3 kg of HDPE assuming the metal structure has a porosity of 90%. Another 15% space is added as a buffer in case the expansion during melting is greater than expected from the available thermal properties data. Container dimensions are shown in figure 4.2.

The top of the container is designed as a removable, flat lid. To assure a tight connection between the container walls and the top lid, a heat package is to be used in the transition between wall and lid and the lid should be fastened with bolts. To account for over pressure, the lid will be equipped with two ventilation holes having non-sealing plugs.

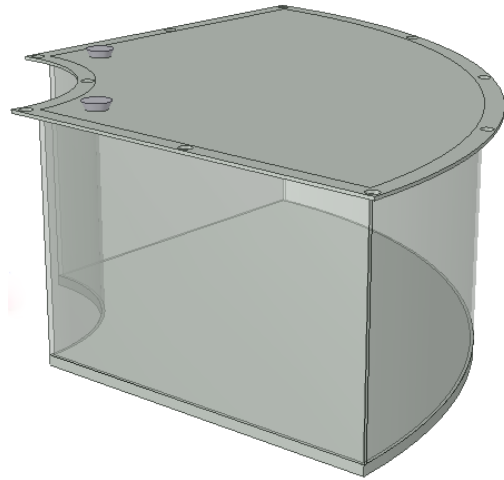


Figure 4.1: Design of a latent heat storage container to be used for experimental testing of combining a LHS with wood stoves.

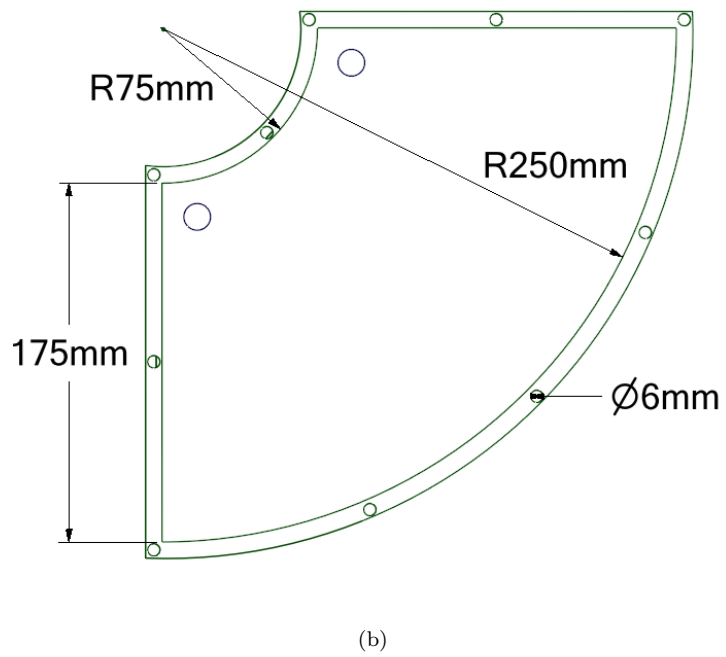
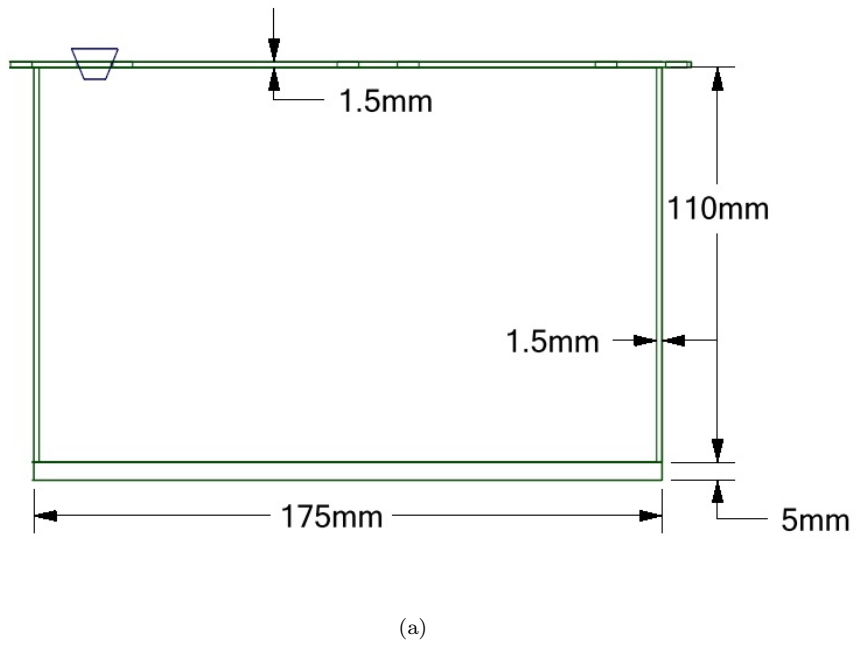


Figure 4.2: Latent heat storage container dimensions (a) side walls (b) bottom plate and top lid.

4.1.2 Metal structure design

Relationship between effective thermal conductivity, melting time and porosity

2D simulations of the first LHS prototype, gives the relationship between effective thermal conductivity and melting time for HDPE shown in figure 4.3. The effect of increasing the effective thermal conductivity is prominent in the interval $k_{eff} = [1, 2]$ W/mK, where doubling the thermal conductivity reduces the melting time by nearly 50%.

Figure 4.4 shows the relationship between porosity and effective thermal conductivity for structures made out of copper ($k_s = 400$ W/mK), aluminum ($k_s = 200$ W/mK), nickel ($k_s = 80$ W/mK) and cast iron ($k_s = 60$ W/mK), calculated using equation 3.1. When the thermal conductivity of the metal is held constant, a linear relationship between porosity and effective thermal conductivity is obtained.

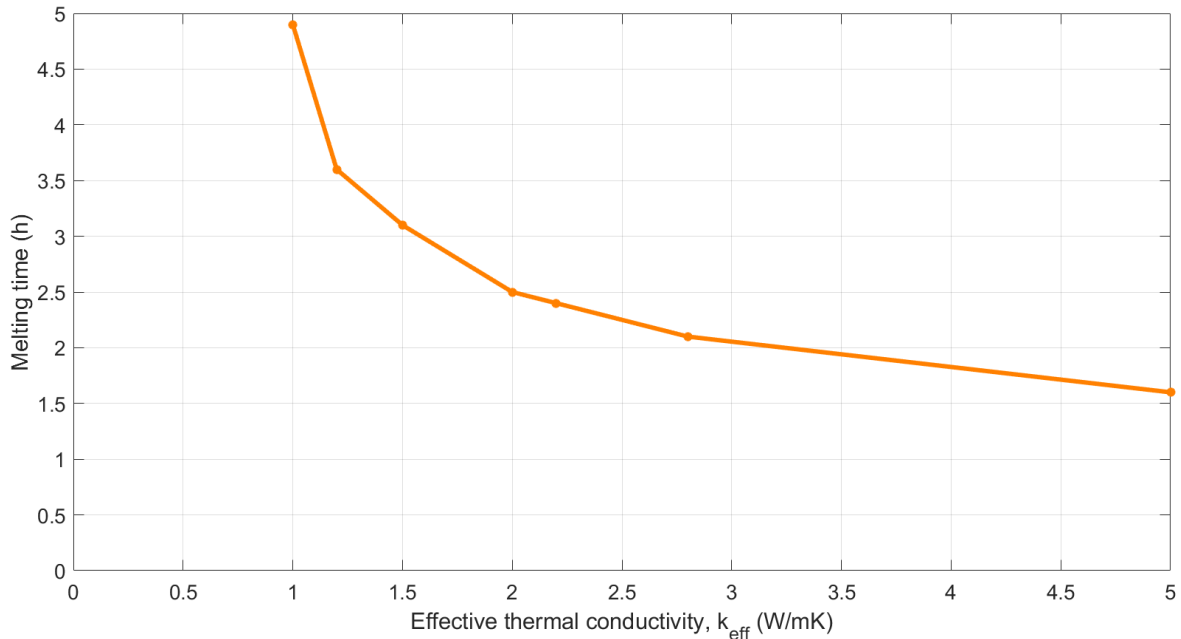


Figure 4.3: An estimated relationship between the effective thermal conductivity of a cellular metal structure/PCM composite and the time it takes to completely melt the PCM. The estimation is based on CFD simulations of a latent heat storage, using the effective thermal conductivities marked by dots.

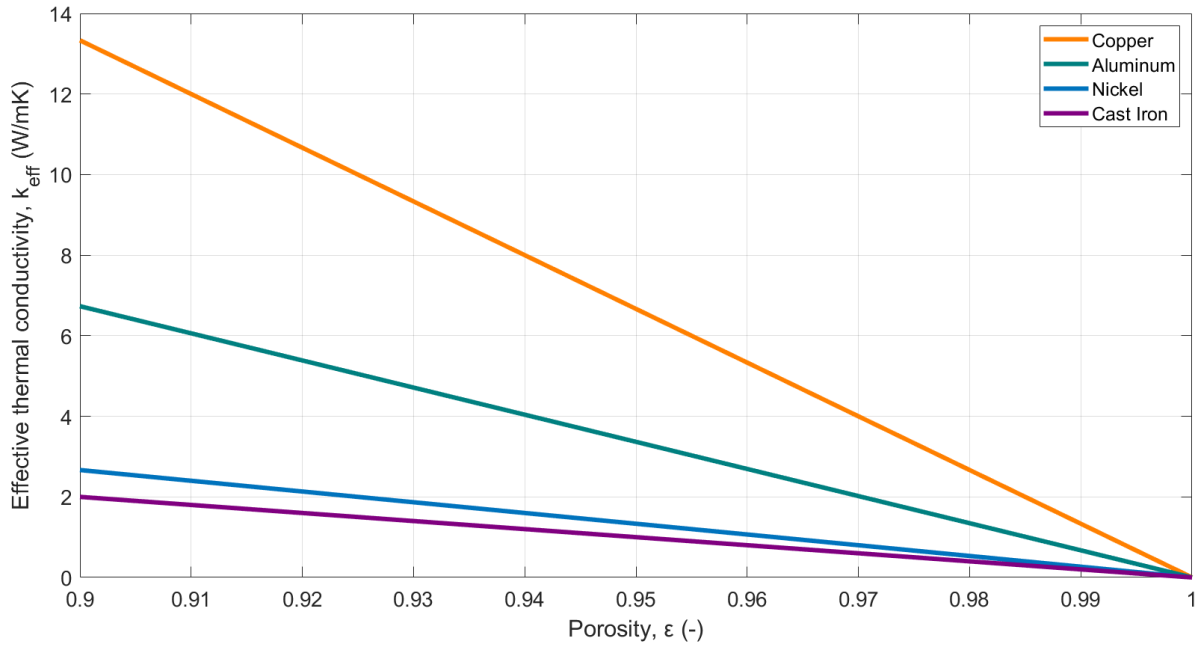


Figure 4.4: Effective thermal conductivity of cellular metal structures made out of copper, aluminum, nickel and cast iron as a function of porosity.

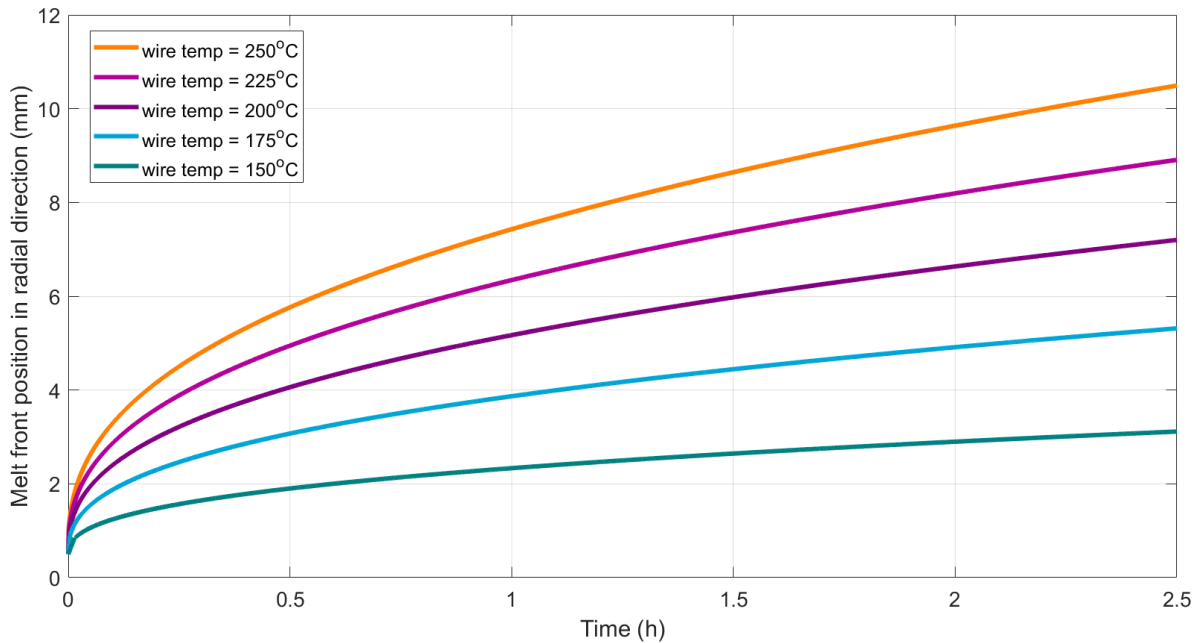


Figure 4.5: An estimation of how the melt front moves in radial direction, with time, in high-density polyethylene surrounding a wire. The wire has a diameter of 1 mm and holds a constant temperature.

Development of the melt front in radial direction

Results from calculations on radial development of the melt front are shown in figure 4.5. Each curve represent the movement of the melt front for a specific wire temperature. Reaching position $r_m = 4$ mm takes less than 30 minutes when the wire temperature is above 200°C. With a wire temperature of 175°C it takes approximately one hour and ten minutes to reach the same position, and more than two and a half hours with a wire temperature of 150°C.

Insight gathered from laboratory tests regarding the behavior of HDPE during phase change

When the temperature of the hot plate was above HDPE melting temperature the material changed appearance from white to clear and the shavings merged into one piece. With increased temperature the material became more uniform and the surface got a smoother finish. However, the material did not become pourable during testing. Figure 4.6 shows the HDPE at different stages in the melting process. In the first frame one can see the original shavings as only a small part of the material has started to melt. In frame three, everything is considered melted. The two bottom frames show HDPE which is cooled down after being melted at 140°C (left) and 220°C (right). A lot of air pockets was observed when examining the solid pieces.

When melted, the material was easy to cut through using a metal spoon holding a temperature higher than HDPE melting temperature. When the temperature of the spoon was at room temperature, the HDPE solidified when it came in contact with the metal. Pushing an aluminum structure in to melted HDPE was unsuccessful. Filling the aluminum structure with solid HDPE shavings resulted in a structure with just a little HDPE and a lot of air. When not pushed together during melting, the material keeps its original shape (shavings) to a greater extent.

Results from research on available metal structures and manufacturing methods

Metal structures are available to be ordered from catalogues online. A range of materials, porosities and pore sizes are available, however, it was difficult finding a structure which had both the desired pore size, porosity and thermal conductivity. Foams and structures are most widely available made out of aluminum. A pore size above 1 cm was rarely found in catalogues. Some suppliers offer to customize the structures. Goodfellow is a company that produces metal foams as well as other metal structures such as meshes and honeycomb structures. Two quotations were received after e-mail correspondence



Figure 4.6: Top row: High-density polyethylene at different stages during melting. Bottom row: Solid high-density polyethylene after being melted at 140°C (left) and 220°C (right).

discussing foam specifications. It was not possible to produce a foam in one piece with the desired dimensions. One quotation offered a foam in eight pieces to the price of 6388.00 GBP. The other quotation was a four piece foam for 2933.00 GBP. All received offers are presented in table 4.1. Further information can be found in the respective appendix specified in the table.

A manufacturing method which allows for greater control of the design of all elements of the structure, is additive manufacturing, or 3D printing. A limitation of this method is the available material from which the structure can be made. The possibility of creating a fitting metal structure using additive manufacturing has been discussed with SINTEF Industry and Tronrud Engineering. The aluminum alloy $\text{AlSi}_{10}\text{Mg}$ is the material with the best thermal conductivity ($\sim 1 \cdot 10^2 \text{ W/mK}$) that either of them can offer. Neither have any experience 3D printing using copper or nickel. To their knowledge, these materials are not yet used for commercial 3D printing. The prices presented in table 4.1 are price estimates received after e-mail correspondence.

Table 4.1: Quotations received March 2020 for the production of a metal structure to be used in the design of a latent heat storage.

Company	Price	Date of quotation	Specifications
Goodfellow	GBP 6388.00 (NOK $\sim 83\ 000$)	11-03-2020	Copper foam, delivered in eight pieces. Details in appendix C.
Goodfellow	GBP 2933.00 (NOK $\sim 38\ 000$)	11-03-2020	Copper foam, delivered in four pieces. Details in appendix C.
SINTEF Industry	NOK $\sim 90\ 000$	24-03-2020	3D-printing a lattice structure with hexagonal cells. Material: $\text{AlSi}_{10}\text{Mg}$. Details in appendix D.
Tronrud Engineering	NOK $\sim 233\ 000$	20-03-2020	3D-printing a honeycomb structure. Material: MS1, $\text{AlSi}_{10}\text{Mg}$. Details in appendix E.

4.2 Results from CFD simulations of case A: A single wire

The purpose of the numerical analysis has been to obtain a better understanding of how heat distributes in a metal structure/PCM composite and how the presence of metal affects the melting process of HDPE. In case A, the focus has been on the effect of the design of different elements of the metal structure, such as wire diameter and pore size. How temperature varies along the wire and how this affects the melting process has also been considered. Simulations have been conducted using models that vary in geometry, boundary conditions and input values, as described in chapter 3.2. An overview of wire material, diameter, temperature and height of structure (for case B) that are used to obtain the results are tabulated in each section.

4.2.1 Effect of wire thickness on PCM melting process

Simulations show that the presence of an aluminum wire shorten the melting process of HDPE and that a thick wire has a larger impact on melting time than a thin wire. Figure 4.7 shows the liquid fraction of the HDPE cylinder with time *without* a wire along the center line and with wires of different diameters. The liquid fraction indicates how big a part of the PCM volume is in liquid state. A liquid fraction of one means the entire PCM volume has melted. For all cases, heat is supplied at a constant temperature of 250°C at the bottom of the cylinder. Background information for the results presented in figure 4.7 can be found in table 4.2.

Table 4.2: Specifications regarding temperature, wire material and diameter used in CFD simulations to obtain results presented in figure 4.7 in section 4.2.1.

Wire material	aluminum
Wire diameter	[0.5, 1, 2]mm
Temperature specifications	constant bottom temp. 250°C

When the entire cylinder is filled with PCM, no wire, a little less than 40% of the PCM is melted after ten hours of heat supply. Implementing a wire of diameter 0.5 mm increases the amount of melted PCM to almost 60% liquid after ten hours. With a wire diameter of 1 mm, the PCM is completely melted after 9 hours and 12 minutes. Increasing the diameter to 2 mm results in a melting time of 2 hours and 36 minutes. A picture of the state of the PCM after one hour simulation flow time is shown in figure 4.8, where the cylinder without a wire is to the far left and the diameter of the wire increases towards the right. The blue color represents solid material, red is completely melted material and the yellow and green shades indicate material in transition between the two phases. With a thicker wire, melting is initiated along a larger part of the wire.

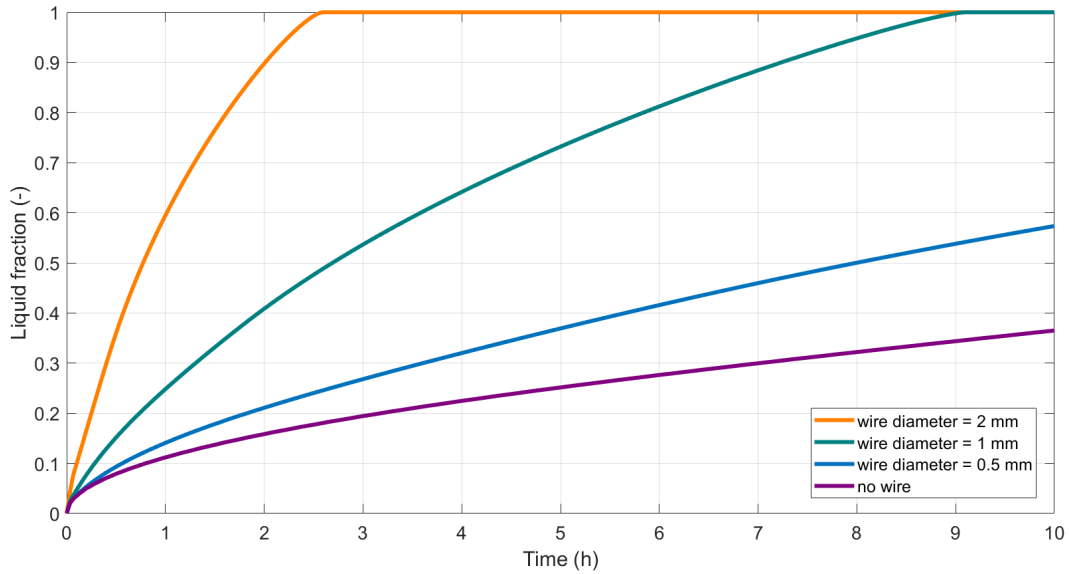


Figure 4.7: Liquid fraction of high-density polyethylene as a function of time. The results are obtained through CFD simulations of a HDPE cylinder with an aluminum wire along the center line. The bottom of the geometry holds a constant temperature of 250°C.

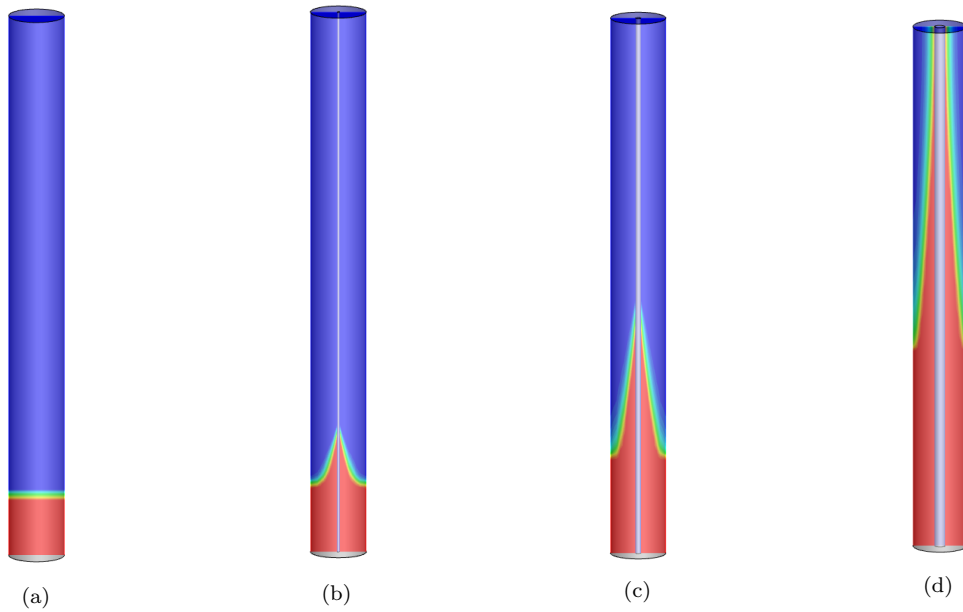


Figure 4.8: The liquid-solid state of high-density polyethylene after one hour simulation flow time, when the bottom of the geometry holds 250°C. Red indicates liquid material, blue is solid and the yellow and green shades indicate material in transition between the two phases. The geometries in figures (b)-(d) have an aluminum wire with diameter d_0 along the center line. (a) no wire (b) $d_0 = 0.5$ mm (c) $d_0 = 1$ mm (d) $d_0 = 2$ mm.

Axial temperature profile and corresponding heat flux function of aluminum wire surrounded by PCM

In figure 4.7, the rate at which the material melts decreases with time. As heat supply to the system is modelled as a constant temperature at the bottom of the geometry, the heat flux decreases with time as the entire system approaches the bottom temperature. Furthermore, the temperature of the wire decreases with position above the bottom plate, which also contributes to slower melting.

The temperature profile of the aluminum wire and how it changes with time is illustrated in figure 4.9 when the wire diameter is (a) 1 mm and (b) 2 mm. The temperature of the 2 mm wire increase faster than the 1 mm wire. The temperature at the top of the wire reaches HDPE melting temperature of 129°C after two hours when $d_0 = 1$ mm, and after 30 minutes when $d_0 = 2$ mm. For the next six hours, the thinner wire has a temperature rise of 13°C at the top. The thicker wire has an equivalent temperature rise over a period of one and a half hours. In both cases, the middle part of the wire has a faster temperature increase than that of the wire top. Following this period, the temperature increase faster towards the bottom temperature of 250°C. After three and a half hours, the temperature of the 2 mm wire is close to uniform.

The corresponding heat flux from wire to surrounding PCM is shown in figure 4.10. The peak heat flux moves upwards along the wire as time passes. As the entire system becomes warmer, the magnitude of the peak decreases. Background information for the results presented in figure 4.9 and 4.10 can be found in table 4.3.

Table 4.3: Specifications regarding temperature, wire material and diameter used in CFD simulations to obtain results presented in figure 4.9 and 4.10 in section 4.2.1.

Wire material	aluminum
Wire diameter	[1, 2]mm
Temperature specifications	constant bottom temp. 250°C

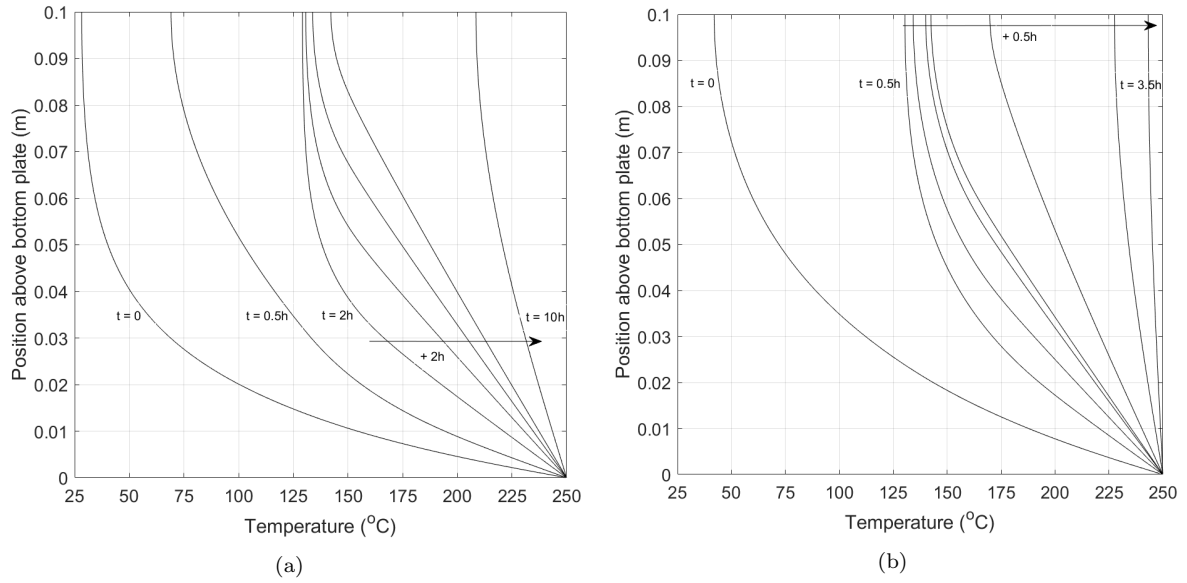


Figure 4.9: Temperature in axial direction of a ten cm aluminum wire with diameter d_0 , surrounded by high-density polyethylene, at different hours after heating is initiated at the bottom of the system. Data are obtained from CFD simulations. (a) $d_0 = 1$ mm (b) $d_0 = 2$ mm.

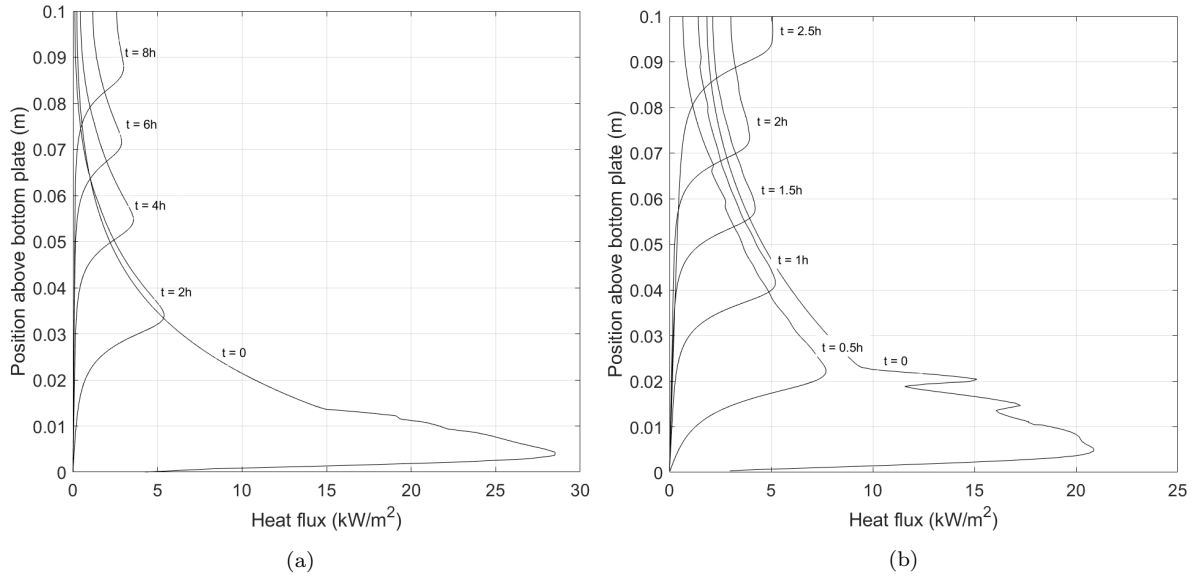


Figure 4.10: Heat flux from aluminum wire with diameter d_0 to surrounding PCM (a) $d_0 = 1$ mm (b) $d_0 = 2$ mm

Melting process of high-density polyethylene surrounding aluminum wire

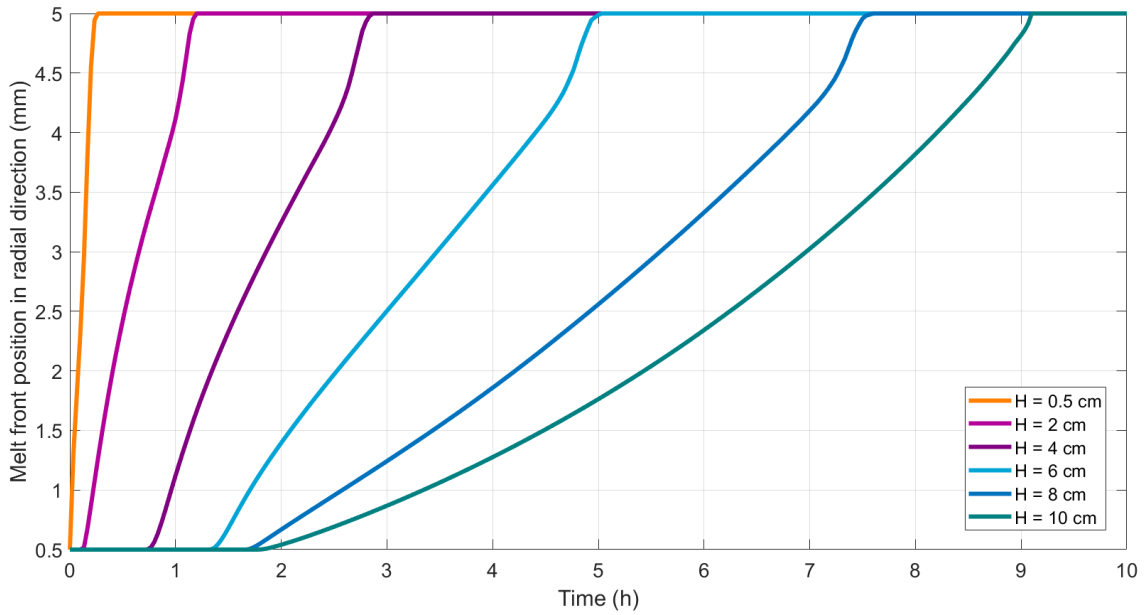
Figure 4.11 shows how the melt front of HDPE moves with time in radial direction at different locations, H , above the bottom of the geometry. The wire diameter is 1 mm and 2 mm in figure (a) and (b) respectively. Further specifications are found in table 4.4. Note the difference in timescale between the two figures. The temperature of the wire as a function of position and time is presented in figure 4.9.

Just above the bottom, at $H = 0.5$, the PCM is completely melted after 14 minutes, when $d_0 = 1$ mm. The melting process becomes more time consuming further away from the bottom. At the top of the system, at $H = 10$ cm, it takes eight hours and ten minutes from the material starts to melt until it is completely liquid. In addition to showing the melt front in radial direction, the figure indicates where the melt front is located in axial direction. After one and a half hours, the PCM is completely melted up to a height of 2 cm, and melting has just been initiated at $H = 6$ cm. Right before two hours have past, melting is initiated along the entire wire. Increasing the thickness of the wire from $d_0 = 1$ mm to $d_0 = 2$ mm, reduces the melting time, especially at the higher levels of the system. Melting the top layer takes two hours and six minutes and melting is initiated along the entire wire within 30 minutes. Figure 4.12 illustrates the solid-liquid state of the system at different hours for both wire diameters.

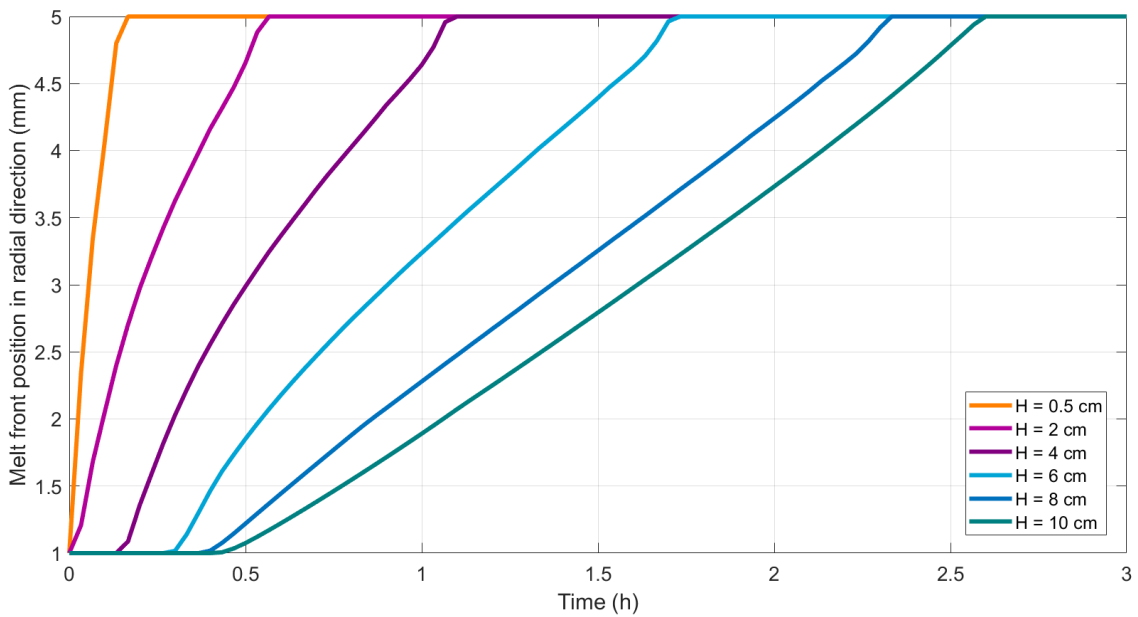
In figure 4.11, the distance between the curves at $H = 8$ cm and $H = 10$ cm deviates from the pattern of the rest of the figure, as does the shape of all the curves between $r_m = 4.5$ and 5 mm. A discussion regarding this can be found in chapter 5.4.

Table 4.4: Specifications regarding temperature, wire material and diameter used in CFD simulations to obtain results presented in figure 4.11 in section 4.2.1.

Wire material	aluminum
Wire diameter	[1, 2]mm
Temperature specifications	constant bottom temp. 250°C

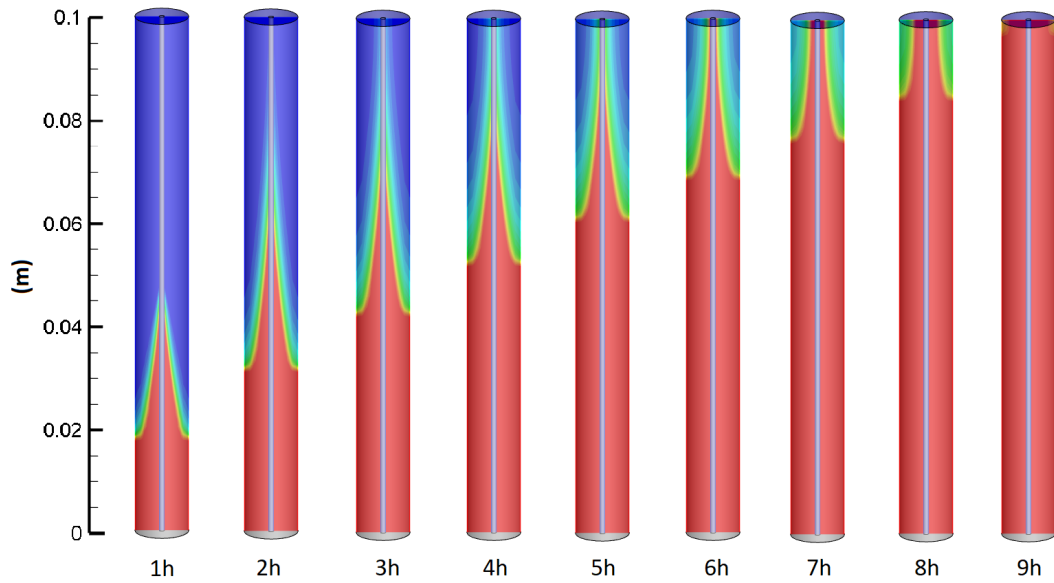


(a)

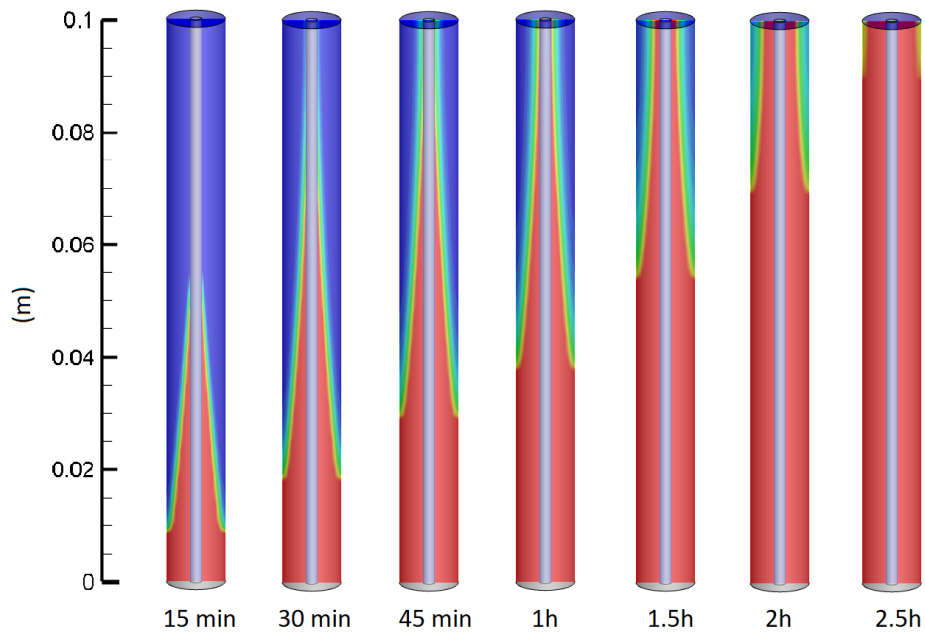


(b)

Figure 4.11: Development of the melt front in radial direction in high-density polyethylene at different positions above bottom plate, which holds a constant temperature of 250°C . The results are obtained through CFD simulations of a HDPE cylinder with an aluminum wire with diameter d_0 along the center line. (a) $d_0 = 1$ mm (b) $d_0 = 2$ mm



(a)



(b)

Figure 4.12: The figures show the liquid-solid state of high-density polyethylene at different hours simulation flow time. Red indicates liquid material, blue is solid and the yellow and green shades indicate material in transition between the two phases. An aluminum wire with diameter d_0 goes along the center line of the cylinder and the bottom of the geometry holds 250°C . (a) $d_0 = 1$ mm (b) $d_0 = 2$ mm

4.2.2 Effect of heat transfer area on PCM melting process

With a larger wire diameter follows a larger heat transfer area between the wire and the surrounding PCM. Figure 4.13 shows how the melt front moves with time in radial direction when the perimeter of the wire is $\pi \cdot 0.5$ mm, $\pi \cdot 1$ mm and $\pi \cdot 2$ mm. The temperature is kept at a constant of 250°C along the entire wire, so that transportation of heat in axial direction is not a factor. Background information for the results presented in figure 4.13 are summarized in table 4.5.

Table 4.5: Specifications regarding temperature, wire material and diameter used in CFD simulations to obtain results presented in section 4.2.2.

Wire material	aluminum
Wire diameter	[0.5, 1, 2]mm
Temperature specifications	constant temp. whole wire 250°C

Simulations show an approximate proportional relationship between heat transfer area and melting time. With the smaller wire diameter of 0.5 mm the melt front is at location $r_m = 5$ mm after 33 minutes. Doubling the heat transfer area reduces the melting time with approximately ten minutes. Doubling the heat transfer area again decreases the melting time with another ten minutes.

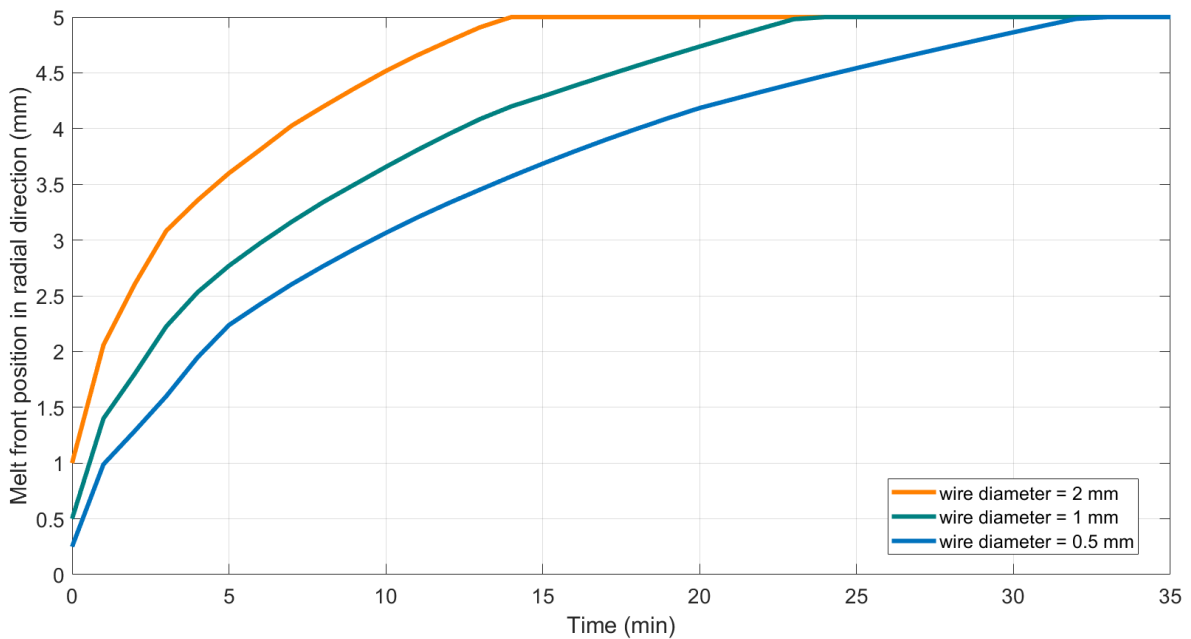


Figure 4.13: The figure shows the effect of heat transfer area on melting time. The results are obtained through CFD simulations of a high-density polyethylene cylinder with an aluminum wire along the center line. The whole wire holds a constant temperature of 250°C , and the curves represent the development of the HDPE melt front in radial direction for different wire diameters.

4.2.3 Effect of wire temperature on PCM melting process

How the melt front moves with time in radial direction for different wire temperatures is shown in figure 4.14. The temperature of the wire is kept constant along the entire wire throughout the simulations and the diameter of the wire is 1 mm. With a wire temperature of 150°C it takes two hours and 24 minutes to melt the PCM all the way to $r_m = 5$ mm. Increasing the temperature by 50°C decreases the melting time by one hour and 43 minutes. Increasing the temperature another 50°C to 250°C reduces the melting time with 17 more minutes. As the radius of the melted PCM becomes bigger, the melt front moves slower in radial direction. Background information for the results presented in figure 4.14 are summarized in table 4.6.

Table 4.6: Specifications regarding temperature, wire material and diameter used in CFD simulations to obtain results presented in section 4.2.3.

Wire material	aluminum
Wire diameter	1 mm
Temperature specifications	constant temp. whole wire [150, 200, 250]°C

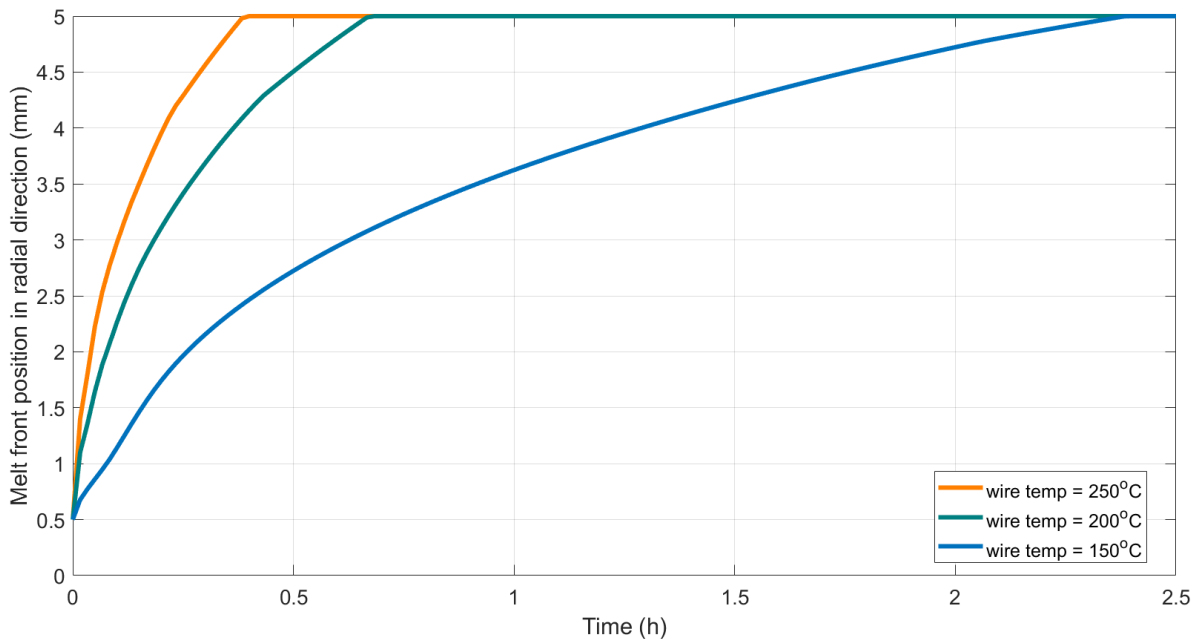


Figure 4.14: The figure shows the effect of wire temperature on high-density polyethylene melting time in radial direction. The results are obtained through CFD simulations of a HDPE cylinder with an aluminum wire with diameter $d_0 = 1$ mm along the center line. The whole wire holds a constant temperature of either 150°C, 200°C or 250°C.

4.3 Results from CFD simulations of case B: Metal structure

In case B, the main focus has been to investigate how heat distributes in a metal structure/PCM composite. How this is affected by what type of metal is used has been examined, as well as how the size of contact area between the structure and the heat source affects the PCM melting time.

4.3.1 Melting process in a 10.8 cm tall metal structure/PCM composite

Figure 4.15 shows the time it takes to melt a section of PCM at different positions, H , above the bottom plate. The sections cut through a cell at its widest point, as marked in figure 4.16. From the time the PCM starts to melt at $H = 0.68$ cm until it is completely melted it takes 23 minutes. The melting time increases with 30 minutes for each section until $H = 4.7$ cm. Completely melting this section takes two hours. From here on up, the melting time of the next section increases faster. The next section, $H = 6.1$ cm, takes another 51 minutes to melt, the one after that 72 minutes more. At $H = 10$ cm the melting time of the section is six and a half hours. Melting is initiated along the entire height of the structure after three hours, and it takes about nine hours to melt all of the PCM. Background information for the results presented in section 4.7 can be found in table 4.7.

Table 4.7: Specifications regarding temperature, wire material and diameter and number of metal structure cells used in CFD simulations to obtain results presented in section 4.3.1.

Wire material	aluminum
Wire diameter	1 mm
Temperature specifications	constant bottom temp. 250°C
No. of metal cells	8

How the temperature varies along the metal structure in vertical direction and how it changes with time is shown in figure 4.17. At position $H = 0$, the temperature is at a constant 250°C. During the first two hours, the temperature of the wire increase rapidly. During the next five hours, the temperature at the top of the wire is close to constant equal the HDPE melting temperature.

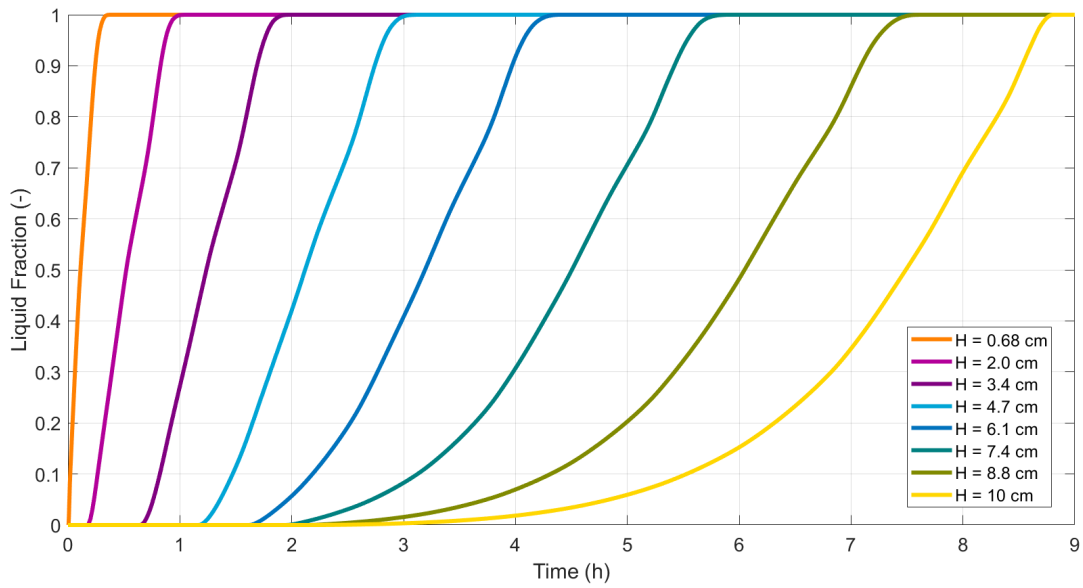


Figure 4.15: Liquid fraction of high-density polyethylene as a function of time at different positions above bottom plate. The results are obtained through CFD simulations of an aluminum structure/HDPE composite with 3% aluminum. The bottom of the geometry holds a constant temperature of 250°C.

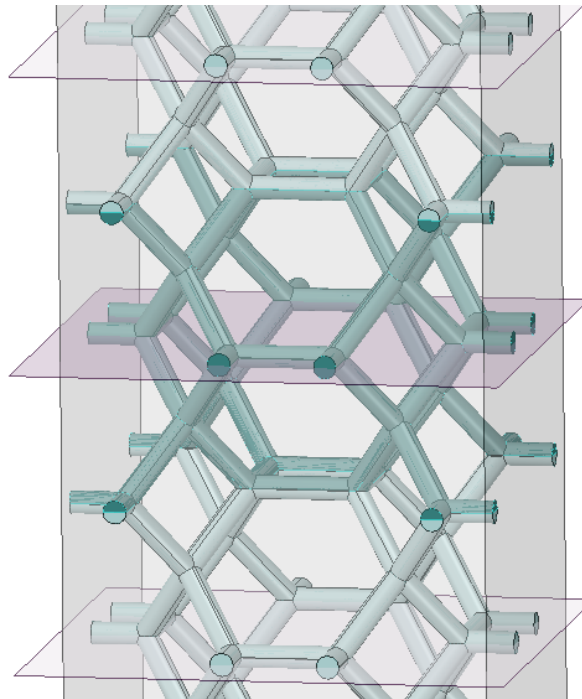


Figure 4.16: A part of an aluminum structure/PCM composite, with section planes marking the widest part of the cells.

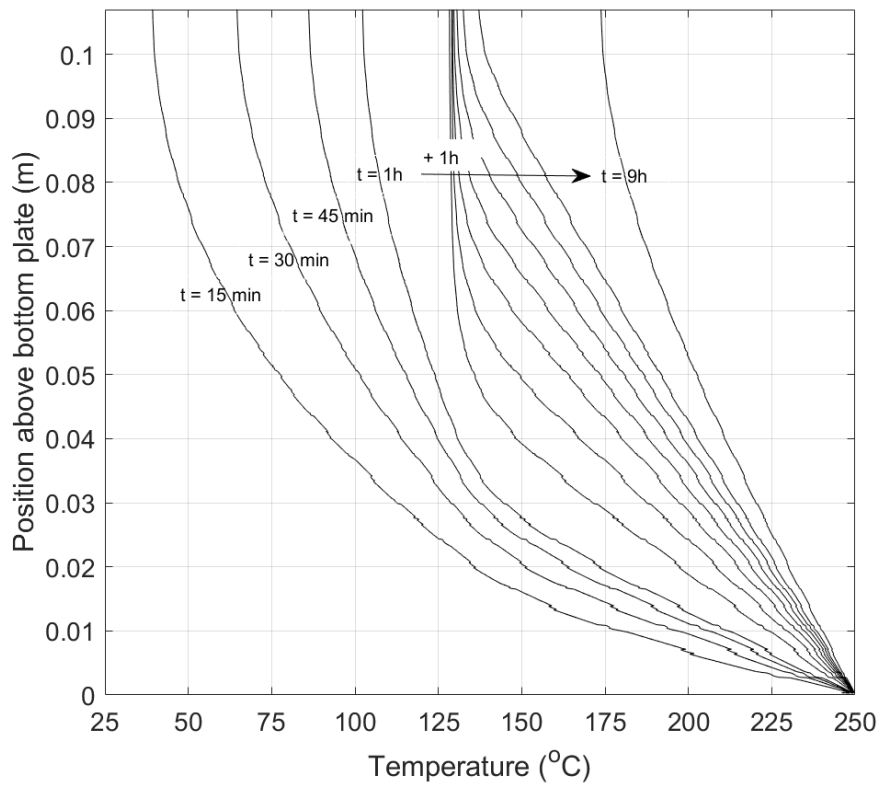


Figure 4.17: Temperature along the wires of a cellular metal structure. The structure is made of aluminum and the bottom of the structure holds a constant temperature of 250°C.

4.3.2 Melting a layer equal the height of one metal cell

An XY-section of the composite contains varying amount of metal and PCM depending on where the section cuts the cells. The time it takes to melt different sections vary, not only depending on position above bottom plate, but also on the metal/PCM distribution of the section. Figure 4.18 shows liquid fraction as a function of time for different cell sections. Data are obtained from simulations of the three cell geometry and further background information is found in table 4.8. The presented results are from the middle cell, located 1.35-2.7 cm above bottom plate. The chosen sections are marked on figure 4.19 and a 2D view of each section after 20 minutes simulation flow time is shown in figure 4.20. The top layer is the most time consuming to melt followed by the middle section.

Table 4.8: Specifications regarding temperature, wire material and diameter and number of metal structure cells used in CFD simulations to obtain results presented in section 4.3.2.

Wire material	aluminum
Wire diameter	1 mm
Temperature specifications	constant bottom temp. 250°C
No. of metal cells	3

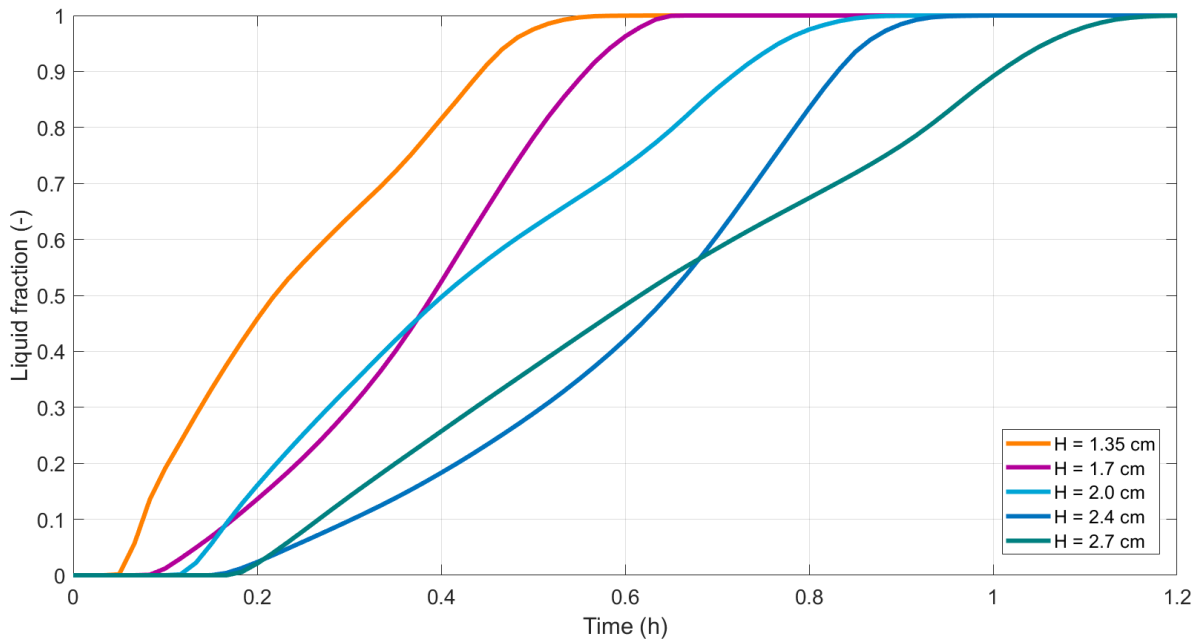


Figure 4.18: Liquid fraction of high-density polyethylene as a function of time at different positions above bottom plate. The results are obtained through CFD simulations of an aluminum structure/HDPE composite with 3% aluminum. The bottom of the geometry holds a constant temperature of 250°C.

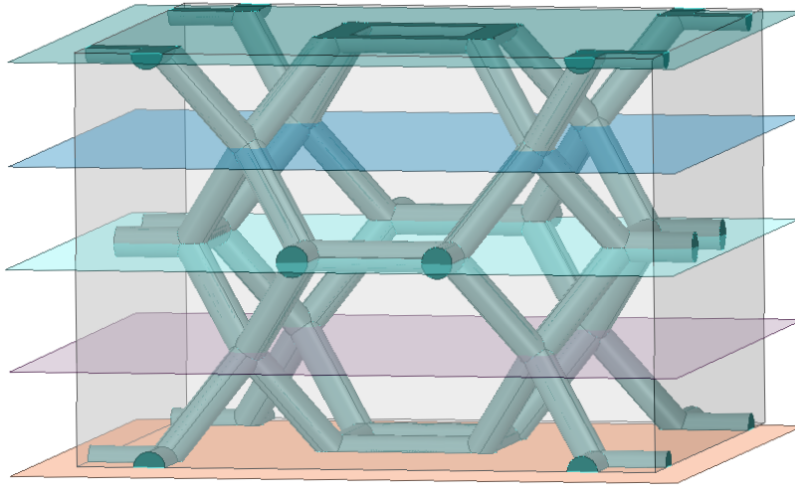


Figure 4.19: One metal structure cell surrounded by PCM with section planes marking the following positions above the bottom of the metal structure/PCM composite: 1.35cm, 1.7cm, 2.0cm, 2.4cm, 2.7cm

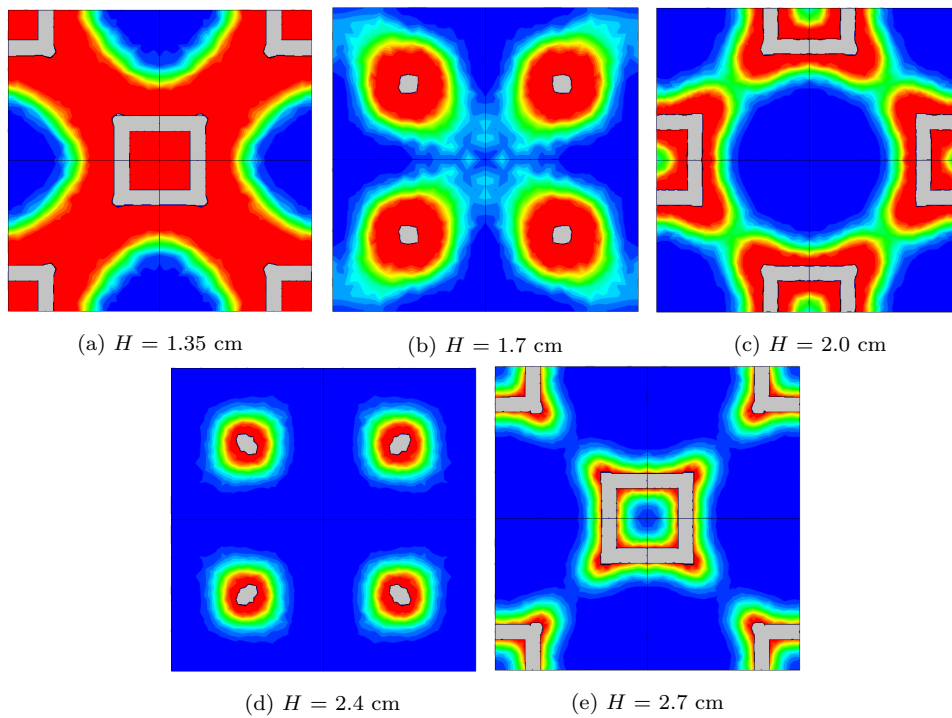


Figure 4.20: XY-sections of a metal structure/PCM composite at position H above the bottom of the composite. The bottom holds a constant temperature of 250°C and the structure is made out of aluminum. The figure shows the liquid-solid state of the sections after 20 minutes heat supply. Blue indicate solid PCM, red is liquid and the yellow and green shades represents material in transition between the two phases. The grey areas are the metal structure.

4.3.3 Effect of metal structure thermal conductivity on PCM melting process

Figure 4.21 shows the difference in PCM melting time depending on whether the metal structure is made out of copper, aluminum or stainless steel. The geometry used for the simulations is that with the height of three cells. Background information for the results are summarized in table 4.9. The melting time is 55 minutes for copper, one hour and 28 minutes for aluminum and seven hours and 21 minutes for stainless steel.

Table 4.9: Specifications regarding temperature, wire material and diameter and number of metal structure cells used in CFD simulations to obtain results presented in section 4.3.3.

Wire material	aluminum, copper, stainless steel
Wire diameter	1 mm
Temperature specifications	constant bottom temp. 250°C
No. of metal cells	3

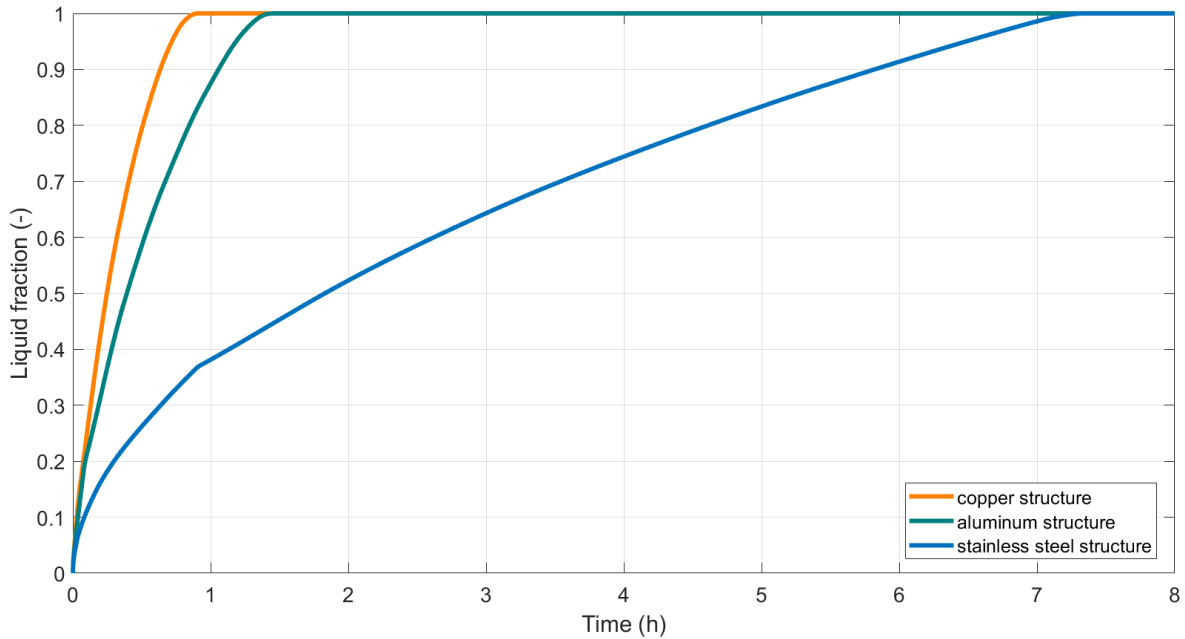


Figure 4.21: The figure shows how melting time of high-density polyethylene differ depending on what type of metal is used in a metal structure/HDPE composite. The results are obtained through CFD simulations of a 4 cm tall metal structure/HDPE composite, where the bottom of the geometry holds a constant temperature of 250°C.

4.3.4 Effect of contact area between metal structure and heat source on PCM melting process

To investigate the consequence of the size of contact area between the metal structure and the bottom plate, simulations with two different metal cell orientations were performed. The cell orientations are illustrated in figure 4.22, where orientation (a) results in a large contact area than orientation (b). A simulation with a layer of 1 mm high-density polyethylene between the structure and bottom plate was conducted to see what happens if no contact is established between the structure and the bottom plate. For this situation, cell orientation (a) was used. Orientation (a) is the orientation used for all previously presented results.

Results are presented in figure 4.23, showing that the melting time is prolonged using cell orientation (b) compared to cell orientation (a). If no contact is established between the structure and the bottom plate, the melting time is lengthened even more. No contact results in a delay especially in the beginning of the heating period. Background information for the results are summarized in table 4.10.

Table 4.10: Specifications regarding temperature, wire material and diameter and number of metal structure cells used in CFD simulations to obtain results presented in section 4.3.4.

Wire material	aluminum
Wire diameter	1 mm
Temperature specifications	constant bottom temp., 250°C
No. of metal cells	3
Contact area between structure and bottom plate	Two different cell orientations: Contact area orientation (a) > contact area orientation (b) No contact: 1 mm HDPE between structure and bottom plate

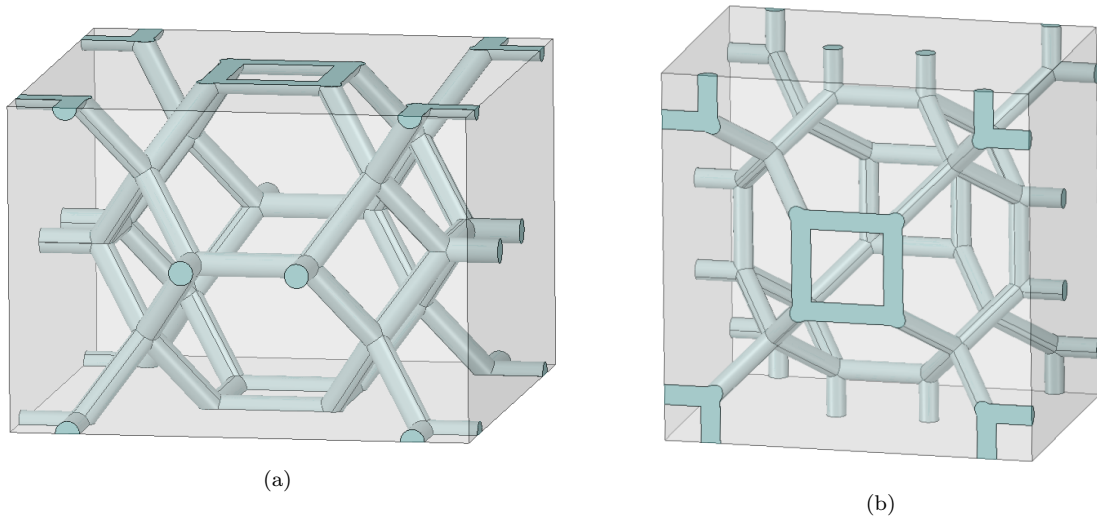


Figure 4.22: Two cell orientations, where cell (a) has a larger contact area with the XY-plane than cell (b).

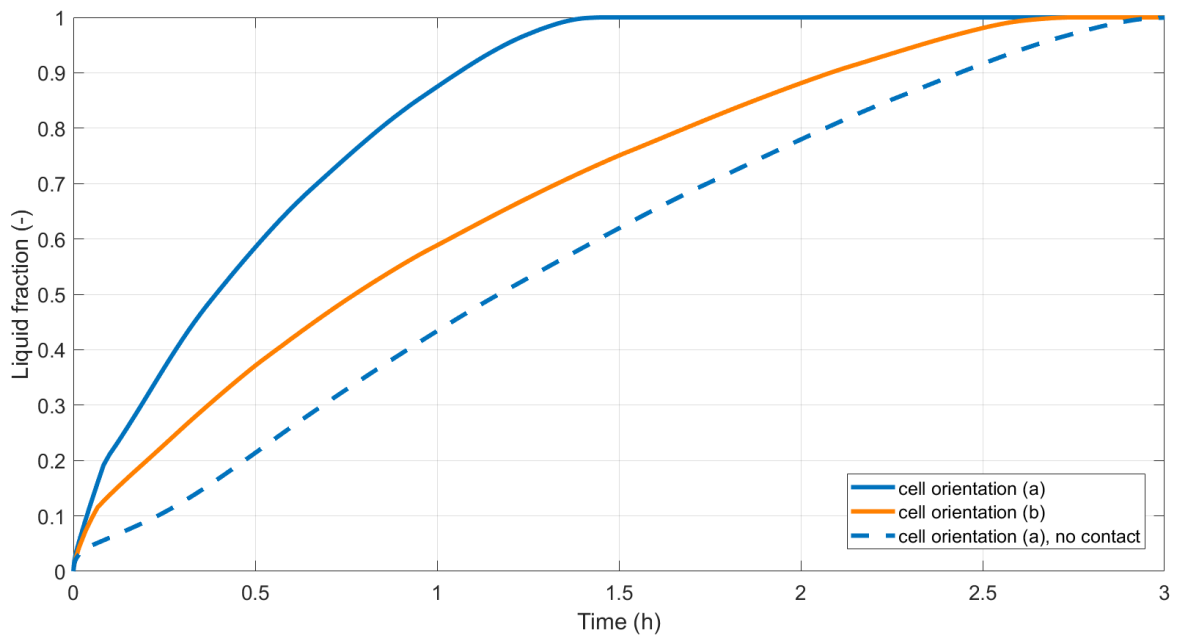


Figure 4.23: The figure shows how melting time of high-density polyethylene differ depending on the size of the contact area between the metal in a metal structure/HDPE composite and the heat source. The results are obtained through CFD simulations of a 4 cm tall aluminum structure/HDPE composite, where the bottom of the geometry holds a constant temperature of 250°C. Two different metal cell orientations were used to obtain differently sized contact areas (orientation (a) > orientation (b)). 1 mm of HDPE was put between the bottom plate and the metal structure to simulate the consequence of no contact between the two.

Chapter 5

Discussion

5.1 Discussion regarding experimental design

The new test design was developed with the main purpose of improving transportation of heat through the PCM and shorten the time of one charge/discharge-cycle. The exterior design of the container was kept similar to the first prototype, with some small adjustments, such as changing the top of the container. During laboratory testing it will be an advantage to be able to take off the top of the container to inspect the melting process, which was not the case with the first prototype. At the same time, it is important to have a tight connection between the top and the container walls to prevent unintended heat loss. Making changes to other aspects of the exterior design such as the material of the container or the thickness of its walls was not considered, as the main focus was on designing a metal structure for improving the heat conduction through the PCM. The shape of the already existing heating plate was a limitation regarding the geometry of the container as it otherwise could have been made simpler and smaller.

5.1.1 Discussion regarding design of metal structure

A design of a metal structure was not finalised, mainly due to questions regarding the practical execution. The number one practical challenge is filling the structure with HDPE. A solution to this problem has not been found. One could perform more laboratory testing trying to supply heat for a longer time and raise the temperature of the material further to see if it becomes more liquid, reheat the same piece of HDPE several times to see if more air disappears and try different methods for supplying heat, not only supplying it from the bottom, to achieve a more uniform melting. However, researching alternative PCMs with a more liquid consistency should strongly be considered, if it is desirable to proceed with using a cellular metal structure for heat transfer enhancement.

Another challenge was finding a suitable material. It is desirable that the material has a high thermal conductivity and can withstand temperatures close to 300°C. Furthermore, it has to be possible to make it into a suitable structure. The materials considered were copper, aluminum, nickel, cast iron and stainless steel. With a higher thermal conductivity, a smaller amount of metal is necessary for achieving an acceptable melting time. Consequently, there is more space for PCM which gives the heat storage a better storage capacity per volume unit. Out of the mentioned materials, copper is the best choice in that matter. Copper structures are available to order from catalogue, but due to the first mentioned challenge of filling the structure, they were all considered unsuitable. Two quotations of custom-made copper foams were received from the company Goodfellow. Details regarding economical aspects of the LHS system has not been considered in this thesis, however, it can be argued that the prices for customizing these structures were expensive.

The second best material regarding thermal conductivity, and thereby storage capacity, is aluminum. Aluminum also provides the most choices; foams, meshes, honeycomb structures and additive manufacturing is more available when choosing aluminum. The limitation of this material is the temperature it can withstand, as it reduces its strength at relatively low temperatures [22]. It was attempted to find exactly what temperature would be the maximum temperature an aluminum structure could tolerate. As this has not been determined it can not be stated whether an aluminum structure is suitable for use in a LHS system for wood stoves.

Nickel and cast iron has lower thermal conductivity than copper and aluminum, hence a lower porosity would be necessary to attain the same decrease in melting time. Based on the results presented in figure 4.3 and 4.4, it can be argued that one should aim to achieve an effective thermal conductivity around 3 W/mK. Increasing the effective thermal conductivity from 3 W/mK to 5 W/mK gives a small reduction in melting time compared to raising the effective thermal conductivity from 1 W/mK to 3 W/mK, while reducing the storage capacity per volume unit equally as much. To achieve an effective thermal conductivity of 3 W/mK using copper, a porosity of approximately 98% is sufficient. With nickel or cast iron the porosity has to be lower than 90%. A lower porosity could be considered had it been accompanied by other benefits, such as more suitable and available structures. That does not seem to be the case with nickel or cast iron, though it should be stated that the focus has been on copper and aluminum structures when researching available structures. The thermal conductivity of stainless steel is too poor for it to be a reasonable material to use in cellular metal structures for heat transfer enhancement.

Based on results presented in figure 4.5 regarding the development of the melt front in radial direction, there is a big difference in melting time depending on the wire temperature. After two hours of heat supply at 150°C, the melt front is at $r_m = 3$ mm.

When the wire temperature is 200°C, the melt front is at $r_m = 6.5$ mm after two hours. To make any conclusions regarding pore size, it is necessary to know what temperature will be at the top of the structure, as this is where the lowest temperature will be. As the numerical analysis showed, this strongly depends on the thickness of the wires. The results presented in figure 4.5 are insufficient for making decisions regarding pore size. The dependency between wire thickness, pore size and porosity will be further elaborated upon when discussing the results from the numerical analysis.

What *can* be stated based on the results of the analytical calculations is that the melt front moves slower in radial direction with time. As the system becomes warmer, the heat flux between the wire and the solid PCM decreases. At the same time, the volume of PCM that is to be melted increases with increasing radius. Furthermore, as the layer of melted PCM between the wire and the solid PCM becomes thicker, a larger thermal resistance appears, which all contributes to a decrease in melting rate.

5.2 Discussion case A

The results from case A will be discussed with respect to wire thickness and pore size. Mathisen operated with a six hour time limit for when the PCM should be completely melted, when evaluating the performance of his latent heat storage design [6]. The same time frame will be used when discussing the results from the CFD simulations.

5.2.1 Wire thickness

The wire with 2 mm diameter, reaches a higher temperature a lot faster than the thinner wires, as the thermal resistance to a larger extent is to be found in the PCM rather than the wire. Melting of HDPE happens at wire temperatures 10-20°C higher when $d_0 = 2$ mm, compared to $d_0 = 1$ mm. The temperature of the bigger part of the wire lies within 130-200°C during the melting period of the PCM. According to the results presented in figure 4.14, this is the temperature range where melting time is the most sensitive to change in heat source temperature. A larger wire thickness is therefore beneficial for obtaining higher temperatures in the metal structure and thereby decreasing the melting time.

A larger heat transfer area has a positive effect on shortening the melting time (figure 4.13). It is desirable to keep the LHS unit lightweight and the storage capacity as big as possible, which favors a large heat transfer area per volume unit metal. The relationship between heat transfer area and volume can be expressed as $2 \cdot \frac{1}{r_0}$. From a purely area-to-volume consideration, a small wire thickness is preferable.

As a thick wire transports heat better in axial direction, the structure can be taller compared to using a thin wire. With a wire diameter of 1 mm, the cylinder should not be taller than approximately 7 cm for it to melt within six hours. With a wire diameter of 2 mm, the 10 cm cylinder melted within three hours and could have been even taller. As the LHS is imagined placed on the top of a wood stove, the base area of the container is limited. To incorporate more PCM and thereby increase the storage capacity of the container, the height of the storage unit is the easiest to adjust. A further investigation of wire diameters above 1 mm of varying length could be interesting, looking to find an optimal combination of wire diameter and structure height, with regards to melting time and storage capacity.

It should be mentioned, as the total volume of metal and PCM was kept constant, increasing the wire radius changed the metal/PCM volume ratio. The geometry with $d_0 = 0.5$ mm contained 0.3% metal, while the geometry with $d_0 = 2$ mm contained 4% metal. However, the calculated reduction in melting time with 2 mm wire diameter is significantly bigger than the decrease of PCM volume, hence increased axial conduction in the metal wire is the main contributing factor for the shorter melting time.

Keeping in mind the desire for a lightweight unit with good storage capacity, a thick wire must be accompanied by a large pore size to attain a satisfying ratio between metal and PCM. Should one choose a thin wire to have a larger heat transfer area per volume, the pore size would need to be smaller. A discussion on pore size follows in the next section.

5.2.2 Pore size

As there is no free convection in melted HDPE, a larger pore size will not be accompanied by the benefit of stronger convection motion, as was found by Lafti et al. [11]. Conduction is the main heat transfer mechanism from which it follows that a small pore will be faster to melt than a big pore. As discussed in the previous section, there are benefits to having a metal structure with thick wires. To attain a satisfying storage capacity, the pore size must be of a certain size. Furthermore, the practical challenge of filling the metal structure with HDPE is believed to favor a large pore size. Therefore, it is of interest to evaluate how big a pore size can be acceptable with regards to melting time.

The results presented in figure 4.14 show that the melt front moves slower in radial direction with time, which is in agreement with the results of the analytical calculations presented in figure 4.5. However, these are results based on constant wire temperatures, which will not be the case during a combustion. The temperature of the wire will change with time and position when heat is supplied from the bottom of the structure. The results presented in figure 4.11 more closely resembles a real situation, where the effect of axial heat conduction in the wire is a factor. The reduction in melting rate with increasing

radius is less prominent and the figure states the importance of good heat conduction in the wire.

To melt the PCM cylinder within six hours, when $d_0 = 1$ mm, the pore radius must be smaller than 2.5 mm, according to figure 4.11a, while the entire cylinder melts within three hours when $d_0 = 2$ mm. A comparison of the combination of 1 mm wire and 2.5 mm pore radius with 2 mm wire and 5 mm pore radius shows that just above the bottom plate, at $H = 0.5$ cm, where the temperature of the wires are approximately the same, a pore of 5 mm is more time consuming to melt than a pore of 2.5 mm. At the top, however, where the temperature of the 2 mm wire is higher than the 1 mm wire, a pore of 2.5 mm is more time consuming to melt.

As the melting time never exceeds six hours when $d_0 = 2$ mm, a maximum pore size for this wire thickness can not be estimated without further calculations or simulations. With a pore size of 5 mm radius and 2 mm wire diameter, the distribution between metal and PCM in a cell structure would be roughly 14% metal and 86% PCM. Whether this is an acceptable metal/PCM ratio is not evaluated in this report.

5.3 Discussion case B

The results from case B will be discussed with regards to porosity and practical challenges incorporating a cellular metal structure to a LHS unit. A discussion regarding set up and limitations of the numerical models will follow in the next sub chapter.

5.3.1 Porosity

The dependency between porosity, thermal conductivity of the metal, melting time and storage capacity per volume unit was introduced in the discussion regarding design of the metal structure in section 5.1.1. To refresh, it is desirable to design a LHS system which can store a substantial part of the heat release during combustion of wood stoves, while keeping the unit compact and lightweight. PCM has a better storage capacity per volume unit than solid metal, which speaks to implementing a metal structure of high porosity. On the other hand, a low porosity has a positive effect on melting time and it does not matter that PCM has a good storage potential if it does not melt within an appropriate time frame. Therefore, one must find a balance between decrease in melting time and decrease in storage capacity.

Results have shown that good upward heat conduction in the metal structure is the main contributing factor for decreased melting time. This can be achieved by using a metal of high thermal conductivity or a structure with thick wires. Highly conducting metals allow for a higher porosity, which gives a better storage capacity per volume unit. The

distribution of metal and PCM in case B simulations was approximately 3% metal and 97% PCM. The results presented in figure 4.21 show that stainless steel is unsuitable for use in cellular metal structures for heat transfer enhancement. Copper and aluminum are promising materials. A discussion regarding availability and concerns about the strength of aluminum, has already been given. A factor that speaks for aluminum, is its low density, compared to copper. In a structure with 97% porosity (which ideally equals 97% PCM, disregarding air in the composite), the density of solid HDPE would be approximately 930 kg/m^3 , the density of copper would be 270 kg/m^3 , while the density of aluminum would only be 80 kg/m^3 . An aluminum structure would add less to the weight of the LHS unit.

However, the results presented in figure 4.15 suggest that 3% aluminum is inadequate for melting a 10.8 cm tall composite within six hours, when the maximum pore width is 14 mm and the wire diameter is 1 mm. Had the composite been 7 cm tall, a 97% porosity would have been sufficient. The bottom area of the LHS test unit is limited to 0.044 m^2 , because of the design of the heating plate. A 7 cm tall structure of 97% porosity, would hold 2.8 kg of HDPE. Based on experience from the preliminary project work, this amount of PCM would not be enough for storing what is considered a substantial part of the wood stove combustion heat release. Whether it is an acceptable amount of PCM for experimental testing of the concept is not considered in this thesis.

As the bottom area of the LHS test unit is limited, the height of the unit becomes important. The structure would have to be taller to contain the same amount of HDPE with a low porosity, compared to a high porosity. Although a lower porosity shorten the melting time, a taller structure increases the melting time. Porosity, wire thickness and thermal conductivity of the structure must be seen in relation to each other when designing a metal structure for heat transfer enhancement.

5.3.2 Practical challenges

In addition to already mentioned practical challenges regarding the consistency of HDPE, available material, cost etc., it is unlikely that a perfect contact between the metal structure and the bottom plate of the LHS container will be possible to attain. Results presented in figure 4.23 show that a layer of 1 mm HDPE between the bottom plate and the structure increases the melting time significantly. Practical challenges that have not been modelled is having an air gap between the PCM and the structure or the consequence of having air pockets inside the PCM.

5.3.3 Heat distribution in a metal structure/PCM composite

Results presented in figure 4.15 show that melting rate decreases with time and position above the bottom plate, as for case A. The temperature of the metal structure decreases in vertical direction, similar to what was seen for a single wire (figure 4.9a). Within a cell, different sections will have different melting patterns depending on the distribution between metal and PCM. The center of a cell is the most time consuming to melt, as this is where the distance between wires is the greatest.

Comparing the melting of a section at position, H , in a cellular metal structure (figure 4.15), with the results from case A, considering the wire of 1 mm diameter (figure 4.11a), melting happens somewhat faster in the cellular structure. A further investigation comparing the increased thermal performance using a cellular structure versus vertical wires, has not been conducted in this thesis. However, it would be interesting to study to what extent the horizontal wires of a cellular structure contribute to reduced melting time compared to taking up space and adding weight to the system. Using vertical wires instead of a cellular structure has the potential to ease several of the practical challenges mentioned. Wires could be welded to the container bottom, establishing good contact for upwards heat transfer in the LHS unit. Using straight wires eliminates the challenge of filling a cell with HDPE, and it simplifies the design of the LHS unit, which can make it easier and cheaper to produce. Further research is necessary before making any conclusions.

5.4 Discussion regarding limitations of the numerical models

The numerical models include simplifications and limitations. All thermal properties, except specific heat capacity, are defined as constant. Adiabatic boundary condition at the top the geometries likely accelerates melting of PCM close to the top. In figure 4.11 and 4.15, melting at the top layer, $H = 10$ cm, happens faster than what would be expected following the pattern of the other curves of the figures. In figure 4.11 the curves have an unexpectedly rapid increase between melt front position $r_m = 4.5$ mm and $r_m = 5$ mm. The adiabatic boundary conditions of the cylinder wall was initially thought to be the explanation, but the same tendency can not be seen in any other results. The boundary condition is likely not the reason in this case, and an explanation for the accelerated increase has not been found.

Heat is supplied to the system by defining a constant temperature at the bottom of the geometry. This places a limitation to available heat flux as a function of time. As commented in the results, this is among the reasons for the decrease in melting rate with time. Raising the temperature of the geometry bottom from room temperature to 250°C

is not a part of the numerical models. To closer resemble a LHS unit being charged by wood stove combustion, the boundary condition at the bottom of the geometry should rather be a function describing the heat flux or temperature development of a wood stove top during a combustion cycle, than a constant temperature.

When creating the models, automatic meshing was used due to limited experience with the ANSYS software. More customized mesh specifications could reduce the computational power and time needed to carry out the simulations, as well as improve the quality of the results. In a redo of the work, more time would be allocated to time step and mesh specifications.

5.4.1 Comparing analytical calculations of melt front development with numerical calculations

The numerical results of case A presented in figure 4.14 aims to represent the development of the melt front in radial direction when the whole wire has a constant temperature. The same goes for the calculations described in chapter 3.1.1. The results of the analytical calculations are compared to the numerical results in figure 5.1, for wire temperatures of 150°C, 200°C and 250°C. The dotted lines represent the analytical results.

The discrepancy between the results are due to simplifications in both the numerical and analytical calculations. A difference between the two approaches is the size and boundary conditions of the control volume. In the numerical model, the control volume is a 10 mm wide cylinder and heat is not allowed to leave the control volume due to the adiabatic boundary conditions. With the analytical approach, the wire is surrounded by an infinite volume of PCM. From this it is reasonable that the results of the analytical calculations show a slower melting than the numerical results. However, when the wire temperature is 250°C, the numerical results show a slightly slower melting than the analytical results, for which a reason has not been unveiled.

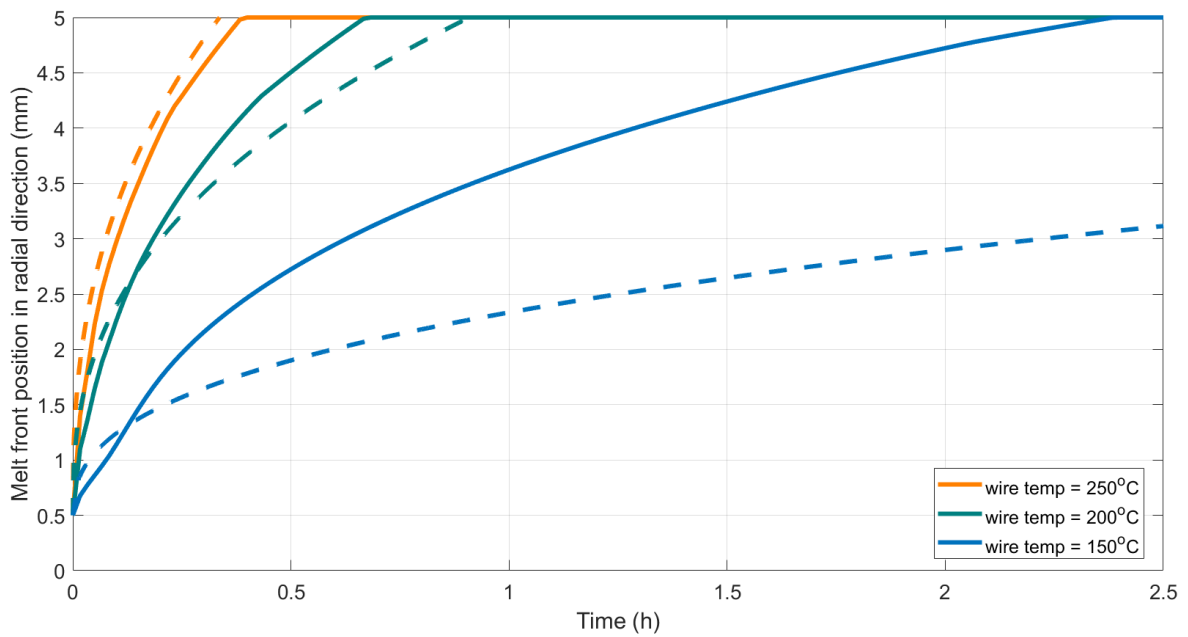


Figure 5.1: The figure shows the result of analytical calculations (dotted lines) and numerical calculations regarding the development of the melt front in high-density polyethylene, in radial direction. The phase change material surrounds a wire of 1 mm diameter, which holds a constant temperature of either 150, 200 or 250°C.

Chapter 6

Conclusion

The objective of this thesis was to explore the potential of utilizing a cellular metal structure as heat transfer enhancement measure for improving the thermal performance of a latent heat storage system. Through a numerical analysis, wire thickness, pore size and porosity of metal structures were evaluated with regards to their effect on heat distribution in metal structure/PCM-composites. The purpose of implementing a metal structure to the latent heat storage system studied in this work, is to enhance the heat conduction inside the storage unit, decreasing the melting time of the PCM. Good upward heat conduction in the metal structure is important to obtain sufficiently high temperatures to melt the PCM at the top of the structure. Results show that the wire diameter to structure height ratio is important in this regard.

Another important contributor to the structures conducting abilities is the thermal conductivity of the structure material. This also affects the storage capacity of the LHS, as a structure with a high thermal conductivity can have a higher porosity and thereby contain more PCM. Out of the materials considered in this thesis, copper or aluminum are the best alternatives with regards to conducting abilities, whereas stainless steel is the worst and is regarded an unsuitable material for this purpose. As the latent heat storage is to be used in combination with wood stoves, it is uncertain whether aluminum is a qualified alternative, as it may not tolerate the temperatures which can occur within the storage.

Pore size must be seen in relation to wire thickness and thermal conductivity of the structure, as the rate at which the PCM melts varies depending on the temperature of the metal structure. Results show that HDPE melting time is sensitive to a change in temperature between 150°C and 200°C. Melting at temperatures below 150°C has not been studied.

The numerical analysis suggests a potential for improving the thermal performance of a latent heat storage system using cellular metal structures. Further calculations and

evaluations are necessary to finalise a design of a structure to be used in the latent heat storage system studied in this thesis. According to the results of the simulations, a cellular structure made out of aluminum with 1 mm wire diameter, 14 mm pore width and a height of 10 cm is insufficient for increasing the melting time of HDPE to an acceptable latent heat storage charge time.

The practical implementation of using a cellular metal structure in combination with high-density polyethylene pose for several challenges, which to a large extent is related to the texture of melted HDPE. It is recommended to investigate alternative phase change materials, having a more liquid consistency. Additional recommendations for further work follows in the next section.

6.1 Further work

- Research alternative PCMs, which have a more liquid consistency when melted. A less viscous material would help with the challenge of filling the cellular metal structure with PCM. Furthermore, if heat transfer by free convection were initiated, it could help speed the melting process.

- Experimental testing of a cellular metal structure/PCM composite.
Why:
 - To gain a better understanding of the heat distribution in such a composite, as the results of the numerical analysis are based on several simplification.
 - To unveil the actual consequences of practical challenges, such as establishing contact between the metal structure and the bottom of the LHS container, from where heat is supplied to the system, and to uncover practical challenges which have not been thought of.

What needs to be done:

- One must find a solution to the challenge of filling the cellular structure with PCM. Two suggestions: 1) Use a different PCM which has a liquid consistency when melted, so that it can be poured into the structure. 2) Continue to explore ways of filling a structure with HDPE.
- The design proposed in chapter 4.1 should be adjusted based on insight gathered from the numerical analysis.
- Find a reasonably priced metal structure, which fits "well enough" with the specifications of the design.

- Further numerical analysis of cellular metal structures.
 - Adjust the boundary conditions of the numerical model.
Why:
 - For the model to more closely resemble a LHS system being charged by wood stove combustion.What needs to be done:
 - Change the boundary condition at the bottom of the geometry from constant temperature to a function describing the heat flux or temperature of a wood stove top during a combustion cycle.
 - Change the boundary condition at the top of the geometry from adiabatic to include heat loss to the surroundings.
 - CFD simulations of cellular metal structures with different combinations of pore size and wire diameter. Wire diameters should be above 1 mm. Pore size must be evaluated relative to storage capacity and melting time.
Why:
 - To design a structure that can provide an acceptable storage capacity and charging time for the LHS system.
- Further investigation of using vertical wires for heat transfer enhancement.
 - Numerical simulations exploring diameter/length ratio for wires.
 - How many wires are necessary? Will cost and manufacturing pose limitations?

Bibliography

- [1] A. Sevault. (Feb. 14, 2017). Pcm-eff. SINTEF, Ed., [Online]. Available: <https://www.sintef.no/prosjekter/pcm-eff/> (visited on 12/02/2019).
- [2] A. Sevault, J. Soibam, N. E. L. Haugen, and Ø. Skreiberg, “Numerical modelling of a latent heat storage system in a stovepipe”, SINTEF/NTNU, Scientific report, Apr. 28, 2018.
- [3] A. Sevault, J. Soibam, N. E. L. Haugen, and O. Skreiberg, “Investigation of an innovative latent heat storage concept in a stovepipe”, SINTEF/NTNU, Scientific report, 2018.
- [4] A. Sevault, H. Kauko, M. Bugge, K. Banasiak, N. E. Haugen, and Ø. Skreiberg, “Phase change material for thermal energy storage in low- and high-temperature applications: A-state-of-the-art”, SINTEF Energy Research, Scientific Report, Nov. 30, 2017.
- [5] A. Sevault, H. H. Mathisen, E. Næss, and Ø. Skreiberg, “Latent heat storage unit integrated on top of wood stoves: Concept design and preliminary cfd modelling”, SINTEF/NTNU, Scientific report, 2019.
- [6] H. H. Mathisen, “Experimental design and testing of a pcm-based heat storage unit for wood stoves”, Master Thesis, Norwegian University of Science and Technology, Sep. 1, 2019.
- [7] S. Lindegård, “Investigation of heat transfer in phase change materials”, Norwegian University of Science and Technology, Project report, 2019.
- [8] N. I. Ibrahim, F. A. Al-Sulaiman, S. Rahman, B. S. Yilbas, and A. Z. Sahin, “Heat transfer enhancement of phase change materials for thermal energy storage applications: A critical review”, *Renewable and Sustainable Energy Reviews*, vol. 74, pp. 26–50, 2017. DOI: <https://doi.org/10.1016/j.rser.2017.01.169>.
- [9] A. Siahpush, J. O’Brien, and J. Crepeau, “Phase change heat transfer enhancement using copper porous foam”, *Journal of Heat Transfer-transactions of The Asme - J HEAT TRANSFER*, vol. 130, Aug. 2008. DOI: 10.1115/1.2928010.

-
- [10] Y. Zhong, Q. Guo, S. Li, J. Shi, and L. Liu, “Heat transfer enhancement of paraffin wax using graphite foam for thermal energy storage”, *Solar Energy Materials and Solar Cells*, vol. 94, no. 6, pp. 1011–1014, 2010. DOI: <https://doi.org/10.1016/j.solmat.2010.02.004>.
- [11] K. Lafdi, O. Mesalhy, and S. Shaikh, “Experimental study on the influence of foam porosity and pore size on the melting of phase change materials”, *Journal of Applied Physics*, vol. 102, no. 8, p. 083 549, 2007. DOI: 10.1063/1.2802183. eprint: <https://doi.org/10.1063/1.2802183>.
- [12] P. Ranut and E. Nobile, “On the effective thermal conductivity of metal foams”, *Journal of Physics: Conference Series*, vol. 547, p. 012 021, 2014. DOI: 10.1088/1742-6596/547/1/012021.
- [13] V. V. Calmidi and R. L. Mahajan, “The effective thermal conductivity of high porosity fibrous metal foams”, *Journal of Heat Transfer*, vol. 121, pp. 466–471, 1999. eprint: <https://doi.org/10.1115/1.2826001>.
- [14] A. Bhattacharya, V. Calmidi, and R. Mahajan, “Thermophysical properties of high porosity metal foams”, *International Journal of Heat and Mass Transfer*, vol. 45, no. 5, pp. 1017–1031, 2002. DOI: [https://doi.org/10.1016/S0017-9310\(01\)00220-4](https://doi.org/10.1016/S0017-9310(01)00220-4).
- [15] R. Singh and H. Kasana, “Computational aspects of effective thermal conductivity of highly porous metal foams”, *Applied Thermal Engineering*, vol. 24, no. 13, pp. 1841–1849, 2004. DOI: <https://doi.org/10.1016/j.applthermaleng.2003.12.011>.
- [16] X. H. Yang, J. J. Kuang, T. J. Lu, F. S. Han, and T. Kim, “A simplistic analytical unit cell based model for the effective thermal conductivity of high porosity open-cell metal foams”, *Journal of Physics D: Applied Physics*, vol. 46, no. 25, p. 255 302, 2013. DOI: 10.1088/0022-3727/46/25/255302. [Online]. Available: 2.
- [17] A. Ahern, G. Verbist, D. Weaire, R. Phelan, and H. Fleurent, “The conductivity of foams: A generalisation of the electrical to the thermal case”, *Colloids and Surfaces A: Physicochemical and Engineering Aspects*, vol. 263, no. 1, pp. 275–279, 2005. DOI: <https://doi.org/10.1016/j.colsurfa.2005.01.026>.
- [18] ANSYS, *Ansys fluent theory guide*, Release 15.0, 2013, pp. 601–609.
- [19] C. Wang, T. Lin, N. Li, and H. Zheng, “Heat transfer enhancement of phase change composite material: Copper foam/paraffin”, *Renewable Energy*, vol. 96, pp. 960–965, 2016.
- [20] P. Zhang, Z. Meng, H. Zhu, Y. Wang, and S. Peng, “Melting heat transfer characteristics of a composite phase change material fabricated by paraffin and metal foam”, *Applied Energy*, vol. 185, pp. 1971–1983, 2017, Clean, Efficient and Affordable Energy for a Sustainable Future, ISSN: 0306-2619. DOI: <https://doi.org/10.1016/j.apenergy.2015.10.075>.

- [21] Y. Kwon, R. Cooke, and C. Park, “Representative unit-cell models for open-cell metal foams with or without elastic filler”, *Materials Science and Engineering: A*, vol. 343, no. 1, pp. 63–70, 2003. DOI: [https://doi.org/10.1016/S0921-5093\(02\)00360-X](https://doi.org/10.1016/S0921-5093(02)00360-X).
- [22] F. Armao. (Jul. 31, 2017). Aluminum workshop: How hot is too hot for aluminum? T. WELDER, Ed., [Online]. Available: <https://www.thefabricator.com/thewelder/article/aluminumwelding/aluminum-workshop-how-hot-is-too-hot-for-aluminum-> (visited on 12/10/2019).

Appendix A

Original thesis description

Background and objective Latent Heat Storage (LHS) represents an interesting concept of temporary thermal energy storage in many applications. Phase Change Materials (PCMs) are used as storage materials and the concept is based on heat absorption when the material undergoes a phase change, usually from solid to liquid, and subsequent heat release when the phase change is reversed. This allows for high energy density and low weight of the storage system compared to traditional sensible thermal energy storage. Though many PCM materials are well documented in the literature, their implementation is still limited due to the complexity of designing suitable interfaces between PCM, heat source and heat sink.

Batch combustion in wood log stoves is a promising application for LHS, due to the transient heat release with high peak values that need to be dampened. The purpose of the master project is to investigate a compact, passive, durable LHS system storing a substantial part of the heat release during domestic batch wood combustion, and effectively releasing the stored heat to the room for an extended period after the last batch. The following tasks are to be considered:

1. Literature review, focusing on
 - (a) Calculation of heat distribution in heterogeneous materials, with the purpose of estimating effective/apparent thermal conductivities of PCMs having embedded metal structures for heat transfer enhancement.
 - (b) Measurement methods of for relevant PCM material properties and at relevant temperatures. The availability of such equipment shall be investigated. If possible, the properties of high-density polyethylene shall be measured.
2. A design of an improved latent heat storage system shall be developed, based on the experience acquired with the first prototype tested in the project work. A key factor in the new design is to improve the heat distribution inside the PCM storage.

3. An experimental program shall be planned and performed on the new PCM storage design, with the purpose of documenting the heat distribution inside the PCM, and the overall heat balance of the system, both during heat storage and heat release modes. The test setup, including instrumentation and data reduction shall be presented, and the results shall be presented and discussed. An uncertainty analysis of the results shall be made. Proposals for further improvements on the LHS performance shall be discussed.
4. Results from selected experiments shall be reproduced by numerical simulations, using the CFD tool ANSYS Fluent. Any discrepancies between the numerical and experimental results shall be highlighted and discussed.
5. Proposals for further work shall be made.

Appendix B

Numerical model from preliminary project work

The following description of the numerical model used to perform 2D simulations during the design process is taken from the report of the preliminary project work [7]:

Simulations recreating the laboratory test were conducted using the CFD software ANSYS Fluent. A simplified 2D geometry was used for modelling the test design. The HDPE is enclosed by a rectangular shaped steel container, insulated on top and on one side. The model was set up by A. Sevault and the boundary conditions were adjusted to fit the lab experiment. ANSYS Fluent uses an enthalpy-porosity method for modelling solidification and melting processes, as described in the Fluent Theory Guide [18].

Thermal properties

Regarding material properties and boundary conditions one setup is used for the heating period and another for the discharge. The thermal properties for HDPE are modelled as constant with the exception of the specific heat capacity, which changes with temperature following a piecewise-linear relation. For the heating period the solidus and liquidus temperatures are set to 129 and 134°C respectively. When simulating the solidification, the solidus temperature is 122°C and the liquidus temperature 125°C.

Boundary Conditions

Heat supply to the system is modelled by defining the temperature of the container bottom plate. Using the measured temperatures from the lab test an expression giving

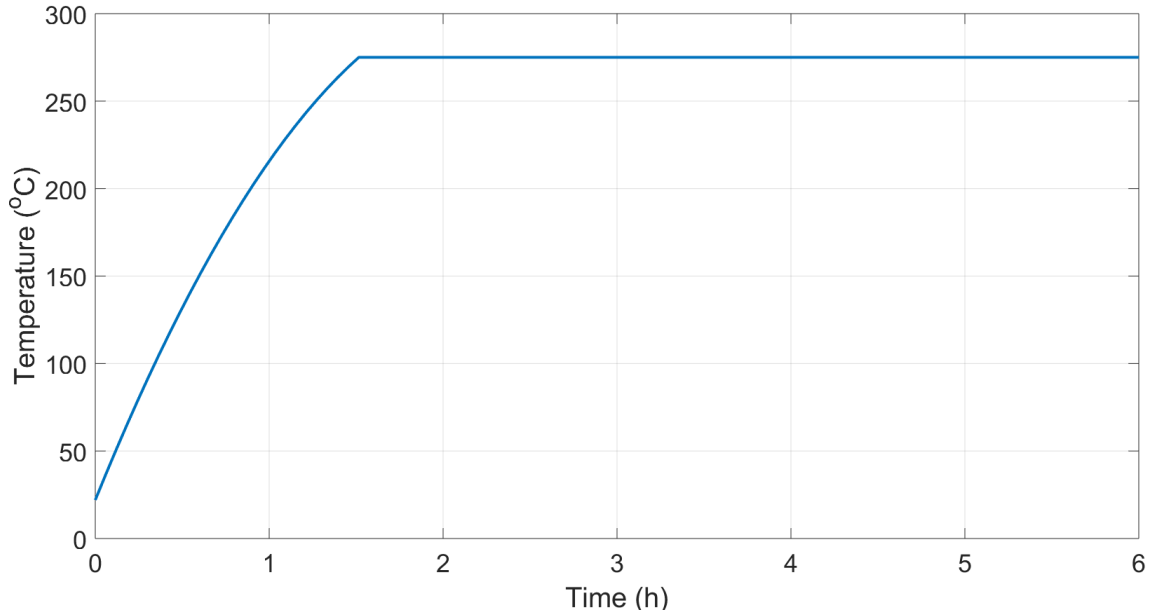


Figure B.1: The temperature development of the container bottom plate used for modelling the energy input of the system in ANSYS Fluent.

the temperature development shown in figure B.1 are defined. During the solidification period, the boundary condition of the container bottom is defined as zero heat flux. The other boundary conditions are the same for heating and cool down. For the insulation surfaces in contact with the ambient air the boundary condition is set as heat transfer by convection with a heat transfer coefficient twice the value of what is assumed to be occurring. This is to compensate for the reduced heat transfer surface of the simplified geometry. The same goes for the uninsulated side wall. Here heat transfer through radiation is also a part of the boundary condition. A contact resistance is defined for the container-HDPE interface to represent the air gap that appears between the two when the HDPE is in solid state [6].

Simulations with melting set up were run for six hours flow time, equal to the heating period for the lab test, followed by solidification for twelve hours flow time. The time step size was set to one second and data were logged every sixth minute. Input data used for the simulations are given in table B.1.

APPENDIX B. NUMERICAL MODEL FROM PRELIMINARY PROJECT WORK

Table B.1: Input data for 2D CFD simulations recreating experimental testing of a LHS.

Property	Unit	Value	Comment
$c_{p, \text{fyrewrap}}$	J/kg·K	700	Specific heat capacity of insulation material.
$c_{p, \text{hdpe liq}}$	J/kg·K	1890-2920	Piecewise linear relation.
$c_{p, \text{hdpe solid}}$	J/kg·K	1890-2920	Piecewise linear relation.
$c_{p, \text{steel}}$	J/kg·K	502	
$\varepsilon_{\text{steel}}$	-	0.9	Emissivity
H	m	0.055	
h_{conv}	m	10	Estimate. Convection heat transfer coefficient.
k_{hdpe}	W/K·m	0.6	Same value for solid/liquid state.
L_s	J/kg	$151.6 \cdot 10^3$	
μ_{hdpe}	Pa·s	1000	Real value unknown.
ρ_{hdpe}	kg/m ³	960	Same value for solid/liquid state.
T_0	K	294.9	
T_{melt}	K	402-407	
T_{solidus}	K	395-398	
T_{surr}	K	295	

Appendix C

Quotation for production of metal foam, Goodfellow

Norwegian University of Science & Technology
NTH Innkjøpsard
NO-9991 TRONDHEIM
NORWAY

Dated 6-March-2020
Our Reference 871109/D E Innamorato
Date 11-March-2020

For the attention of: Sara Lindegard
Our quotation reference : Q1003493

Thank you for your enquiry referenced as above. We have pleasure in offering subject to our standard conditions of sale and without engagement as follows:

1. 90°Segments of copper foam Cu 99.9% to drawing
Condition : Thickness made up of 8 layers trimmed and stacked
Average ppi : +/-20
Average Poresize : Ø1.4
Thickness : 77.0 mm
Width : 177mm

Quantity : 1 lot Price : GBP 6388.00 (Lot)

2. 90°Segments of copper foam Cu 99.9% to drawing
Condition : Thickness made up of 4 layers trimmed a stacked
Average ppi : +/-20
Average Poresize : Ø1.4

APPENDIX C. QUOTATION FOR PRODUCTION OF METAL FOAM,
GOODFELLOW

Thickness : 77.0 mm

Width : 177 mm

Quantity : 1 lot Price : GBP 2933.00 (Lot)

Tolerances: Unless specified above our standard tolerances are :

Despatch forecast 2 weeks after receipt of order. Terms of despatch: Free delivered excluding import duty and tax.

Terms of payment: Net 30 days.

Quote Validity: 30 days from date of issue unless otherwise stated. Goodfellow reserves the right to amend the above quotation within the validity period where commodity prices fluctuate +/-5%

Please note that

Item 1 : Please note, we can not supply 1 pcs according to the drawing, but we can supply 8 layers of thinner layered foam together in one stack.

Leadtime around 5 weeks.

Item 2 : Alternatively, please note, we can not supply 1 pcs according to the drawing, but we can supply 4 layers of thinner layered foam together in one stack.

Leadtime around 7 weeks.

Appendix D

Metal structure specifications discussed with SINTEF Industry

Manufacturing method: 3D printing using SLM280 printer.

A description of the geometry discussed with SINTEF Industry follows on the next page (text in Norwegian).

SINTEF Industry's reply regarding the cost of creating such a geometry:

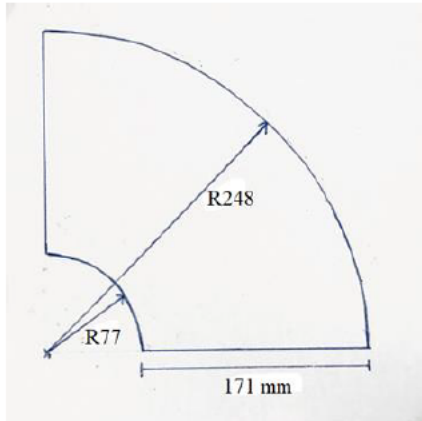
"Printer rates is 1000 NOK/h, we charge real hours. The piece will be around 85mm high (80mm piece + supporting), and each layer there are many features/surface. My limited experience tells it may need 70 hours to print it. Plus some operator hours and powder cost, may be 15000 NOK. Once we have the real 3D model, we could calculate the hours more accurately by the printer computer."

Metal lattice structure

Formålet med metallstrukturen er å øke varmeledningen gjennom et materiale med dårlig termisk konduktivitet.

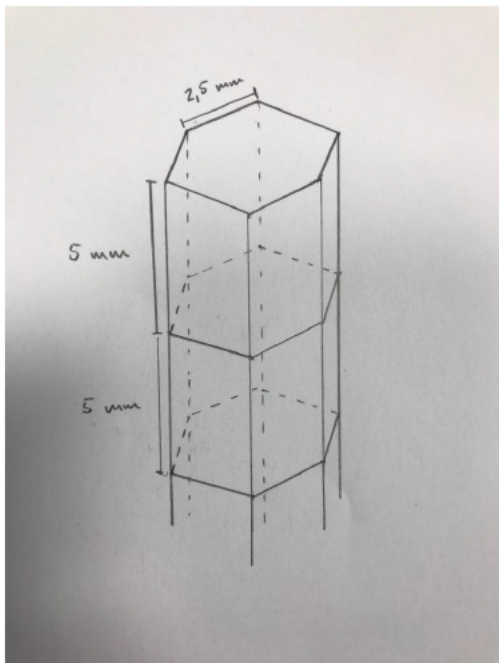
Materiale: $\text{AlSi}_{10}\text{Mg}$

Grunnflaten med mål er illustrert i figur 1. Høyden skal være 80 mm.

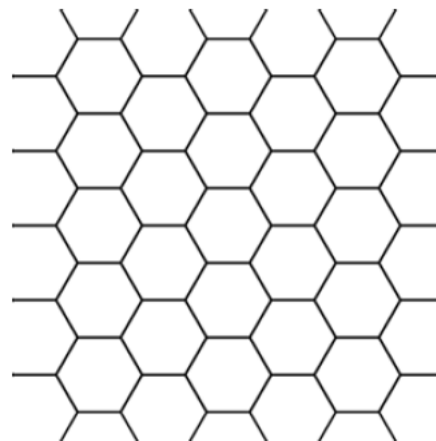


Figur 1: Grunnflate

Ønsker heksagonalformede celler, men andre geometrier kan diskuteres dersom det er utfordrende. Mål på cellene er markert på figur 2. Dette er innvendige mål. Tykkelsen på metalltrådene bør være mellom 0.5 og 1 mm.



Figur 2



Figur 3: Cellestruktur sett ovenfra

Appendix E

Metal structure specifications discussed with Tronrud Engineering

Tronrud Engineering's reply regarding the cost of creating a metal structure with the design shown in figure E.1, using 3D printing (text in Norwegian):

Da har jeg fått skissert en rask modell og simulert til deg. Jeg hadde håpet på at laseren i maskinen ikke skulle trenge å sintre så mye med så små hull, men det viste seg i simuleringen at produksjonstiden ligger rett under 300 timer i MS1.

Med 16 kapp på 5mm må gitteret bygges 32mm over original høyde da sagbladet er 2mm.

Det spørs derfor om additiv tilvirkning er rett måte å lage denne på mtp på pris.

MS1:

- Cad modellering: 4400,- NOK eks moms
- Additiv tilvikning: 225.000,- NOK eks moms
- Oppdeling - 16 kapp, 5mm: 3200,- NOK eks moms

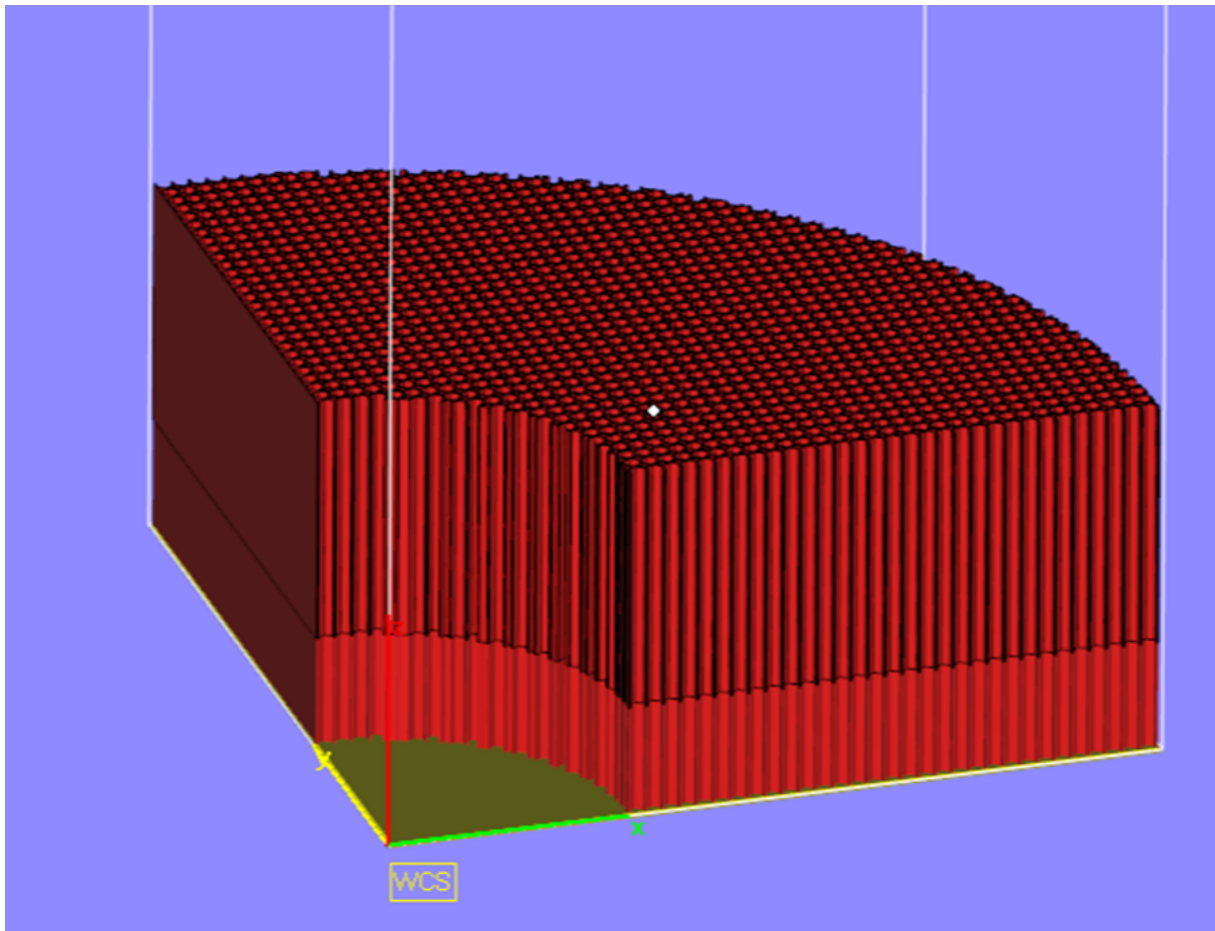


Figure E.1: CAD model of metal structure for 3D printing made by Tronrud Engineering.

